Algal Research 16 (2016) 434–448

Contents lists available at ScienceDirect

Algal Research

journal homepage: www.elsevier.com/locate/algal

Characterization of salt stress-induced palmelloids in the green alga, *Chlamydomonas reinhardtii*

Dolly K. Khona [a], Seema M. Shirolikar [b], Kanak K. Gawde [a], Erik Hom [c], Manjushree A. Deodhar [d], Jacinta S. D'Souza [a,*]

[a] UM-DAE Centre for Excellence in Basic Sciences, University of Mumbai, Kalina campus, Santacruz (E), Mumbai 400 098, India
[b] Department of Biological Sciences, Tata Institute of Fundamental Research, Homi Bhabha Road, Mumbai 400 005, India
[c] Department of Biology, University of Mississippi, 401 Shoemaker Hall, University, MS 38677-1848, United States of America
[d] K. E. T's V. G. Vaze College of Arts, Science and Commerce, Mulund (E), Mumbai 400 081, India

ARTICLE INFO

Article history:
Received 13 August 2015
Received in revised form 18 March 2016
Accepted 27 March 2016
Available online 22 April 2016

Keywords:
Algae
Salt tolerance
Stress
Exopolysaccharides
Palmelloid
iTRAQ

ABSTRACT

Chlamydomonas reinhardtii is a model, free-living, soil and freshwater alga with unicellular vegetative cells under favourable growth conditions. When exposed to certain stress agents, however, *C. reinhardtii* forms multicellular aggregates known as "palmelloids." This study characterizes palmelloid formation in response to sodium chloride (NaCl) salt stress and probes the role of proteins from the spent medium in this process. Detailed morphological and biochemical analysis of NaCl-induced palmelloids of *C. reinhardtii* were carried out along with quantitative mass spectrometry-based protein analysis of stress and post-stress spent media. Exposure to NaCl concentrations of 100 and 150 mM (equivalent in saline soils) induces palmelloid formation and withdrawal of this stress causes rapid dissociation of these clusters. Heterogeneity in cell size and cells with excised flagella remnants within palmelloid clusters suggests heterogeneous cell cycle arrest during palmelloid formation. Additional hallmarks of palmelloidy include: intracellular starch and lipid accumulation and the presence of an extracellular polysaccharide envelope. Analysis of proteins from the spent media of stressed and post-stress conditions implicated involvement of cell wall proteins in palmelloid formation and maintenance and peptidase and flagellar proteins in palmelloid dissociation. With this report, the relevance of NaCl, as a probable environmental cue for driving unicellular, free-living *C. reinhardtii* cells into a multicellular, palmelloid stage is discussed.

1. Introduction

The changing environment of organisms induces tremendous stress on them; the latter being broadly classified as biotic (pathogenic infections, hormones and biotoxins released from these pathogens) and abiotic (the xenobiotics, pesticides, herbicides, fungicides, thermal shock, drought, hypersalinity, radiations, heavy metals and air pollutants). The type, strength and duration of exposure to the stress play an important role in an organism's protective or destructive response towards it. When challenged with biotic/abiotic stress, cell's primary response is to trigger the pro-survival signalling pathways and exhibit an adaptive physiological response for their survival. If this mounting defence response and pro-survival strategy fails, the cell programs itself to die.

Among unicellular soil-inhabiting microorganisms, the most common strategy for survival is the formation of spores/cysts [69]. Under stress conditions, many bacteria undergo asymmetric cell division resulting in the formation of a metabolically inactive daughter cell/spore [70] or exist as vegetative cells with lower metabolic rates for a long period [27]. Many bacteria become transiently 'non-culturable', yet viable with detectable metabolic activity when challenged with stress [46]. Alternately, unicellular, planktonic organisms start living as multicellular communities known as biofilms wherein the cells form an adherent layer on a surface and are enclosed in a self-secreted exopolysaccharide matrix (EPSM, [11]). Of the several single-celled eukaryotes, the green chlorophyte *Chlamydomonas reinhardtii* is preferred as a vital system in studying stress-inducible responses for two main reasons. First, it harbours a host of such stress-responsive genes; but, their functional significance in altering the metabolism for adaptation remains unexplored and second being the ease with which the physiological changes occurring in the cell *vis-à-vis* the stress can be studied [19,36]. It has been used to study responses to various abiotic stress agents such as osmolytes, temperature, irradiation, nutrient starvation, heavy metals and oxidative stressors [17,34,39,58,67,68,73,82]. Being versatile, it displays varied responses to different stress conditions. The physiological changes accommodated by the cell, in response to stress, have been well studied using extensive microscopic methods; while, the recent use of high-throughput techniques such as microarray analysis, RNA sequencing, mass spectrometry, two-dimensional gel electrophoresis, quantitative proteomics with Isobaric tags for relative

* Corresponding author.
E-mail address: jacinta@cbs.ac.in (J.S. D'Souza).

http://dx.doi.org/10.1016/j.algal.2016.03.035
2211-9264/

and absolute quantitation (iTRAQ) have helped in dissecting the molecular players orchestrating these responses. When subjected to stress, the first and instant response is either flagella paralysis or loss [21,62]; [56]; a later response being either 'palmelloid formation' [23,24,38,49, 53] and/or apoptosis [44,67,68,83].The state of palmelloid formation in the genus *Chlamydomonas* is interesting as a study since this organism being 'free-living' (under favourable conditions) programs its entry into a temporary 'colonial-like' stage (under stress) accompanied by following characteristic physiological changes [35,48,49,76]:

(a) exopolysaccharide secretion,
(b) clustering of cells (varying in number; minimum count being a two cell cluster),
(c) cells embedded in the EPSM surrounded by a common membrane,
(d) individual cell wall thickening, and
(e) abnormal cell division.

These morphological changes resemble the morphology of *palmella* in Tetrasporales [66]. The earliest studies on palmelloidy in the *Chlamydomonas* genus were reported in *C. reinhardtii* wherein palmelloidy was induced by exposure to various organic acids [22]. An extension of this study showed that palmelloids were formed in the medium devoid of calcium or when supplemented with EDTA [23]. Furthermore, these palmelloids were found to dissociate in normal growth medium, distilled water or calcium chloride solution [23]. Taking cues from these studies, the effect of chloroplatinic acid (a soluble platinum compound) on cell division and morphogenesis was assessed by Nakamura and co-workers [49]. Palmelloidy was induced in *Chlamydomonas eugametos* in response to chloroplatinic acid [49]. Multiple layers of cell walls in these palmelloids suggested that probably the cells continue to divide in the mother cell i.e. they are unable to separate after division and remain encased in a common membrane. Additionally, it was shown that Tris-buffered medium or the presence of polyfunctional nitrogen compounds in the growth medium suppressed chloroplatinic acid-induced palmelloid formation [48]. Palmelloids were formed in chemostat cultures of *C. reinhardtii* under phosphate limitation [53]. Their growth rate was slower as compared to the vegetative cells in the population; but, they had higher ratio of endogenous polyphosphates to total phosphate as well as the absence of alkaline phosphatase activity. Growth medium with acidic pH of 3.4 and 4.4 was found to induce palmelloidy in *Chlamydomonas applanata* cells [76]. This was accompanied with physiological changes such as decreased cell volume, abnormal cell division, reduction in starch reserves and excessive mucilage secretion. Concomitantly, cell viability was found to be inversely proportional to the stress dose. *C. reinhardtii* cells were reported to form palmelloids when cultured together with a rotifer, *Brachionus calyciflorus*, as a defence mechanism to escape grazing by increasing the particle size [38]. Microarray analysis of paraquat-treated *C. reinhardtii* palmelloids showed differential regulation of genes involved in oxidative stress defence mechanisms indicating the co-ordination of genotypic and phenotypic alterations for cell survival [24].The effect of high salt concentration on *C. reinhardtii* photosynthetic apparatus showed that palmelloids were formed by addition of NaCl in the growth medium [51]. With respect to cell motility in a palmelloid state, different species of *Chlamydomonas* respond differently to stress conditions; the outcome being either loss of flagella or reduction in motility. Transmission electron microscopy analysis of *C. eugametos* palmelloids showed that although the flagella depicted no abnormalities at the ultrastructure level, cell motility was inhibited [49]. Severing of flagella led to compromised motility in *C. applanata* palmelloid cells [76]. Loss of flagella preceded palmelloid formation in *C. reinhardtii* cells when cultured with the rotifer *B. calyciflorus* [38].The phenomenon of palmelloidy in *C. reinhardtii* has been studied as a stress-inducible response. Though a few physiological hallmarks associated with this stage have been considered, the possibility of other such morphological alterations cannot be ruled out. Also, the biochemical changes accommodated by these cells are unknown. Hence, the present study is an attempt to gain insights into palmelloidy at the ultrastructural and biochemical level.

2. Materials and methods

2.1. Materials

Reagents and media components were obtained from Amresco (USA), SRL (India), HiMedia (India), Sigma and Merck (India).

2.2. Methods

2.2.1. Chlamydomonas culture growth and maintenance

The *C. reinhardtii* wild type (WT) strain *cc125* (*Chlamydomonas* Centre, Duke University, Durham, NC, USA) used for all the experiments was cultured and maintained [18,28].

2.2.2. Exposure to stress conditions

C. reinhardtii cells were grown in TAP medium as batch cultures until they reached 1–2 × 10^6 cells/ml (corresponding to mid-exponential phase of growth). The cells were cultured at continuous illumination of 300 μmol/m^2 s. For H_2O_2 (2 mM), Menadione (5, 10 and 15 μM), LiCl (10, 20 and 40 mM), NaCl (50, 100, 150, 350 and 500 mM), sucrose (100, 200 and 300 mM) stress conditions, 25 ml of cells was spun at 1100 *g*/5 min/25 °C; washed with 10 ml of fresh medium followed by re-suspension in fresh TAP with respective concentrations of the stress agents. For acidic (4 and 5) and alkaline (8 and 9) pH, cells were re-suspended in TAP adjusted to the respective pH. For temperature stress, the cells were incubated at different temperatures such as 7 °C/15 °C/ 37 °C/40 °C. A parallel set of cells that were unexposed to any of the above stress conditions served as the experimental control for all assays mentioned further. All these experiments have been conducted thrice with two technical replicates used for each attempt.

2.2.3. Spot viability assay and morphological observations

To assess the viability, 2 × 100 μl of stress-exposed cells were harvested after respective time intervals (0, 1, 6, 18 and 24 h for NaCl, LiCl and sucrose stress; 0, 1, 3, 6, 18 and 24 h for alkaline pH and Menadione stress; 0, 1, 2 and 3 h for temperature stress; 0, 1, 2, 3, 18 and 24 h for H_2O_2 stress; 0, 15, 30 min and 1 h for acidic pH stress) followed by washing and re-suspension in 100 μl fresh medium. 10 μl of these cells (in duplicates) was spotted onto agarified TAP and incubated under routine growth conditions. Plates were checked for viability after 5 days. The spot viability experiment was repeated three times. A representative spot for each treatment has been used to depict in the Supplementary Figure 1.

To assess the morphological changes such as difference in cell size, vacuolation, pigmentation, plasmolysis, chlorophyll bleaching or structural abnormality in any organelle manifested under various stress conditions, 500 μl of the above cells was harvested, washed in 1× Phosphate-buffered saline (PBS, pH 7.0), fixed for overnight at 4 °C in 1× PBS containing 0.75% formaldehyde, washed, re-suspended in 1× PBS. Microscopic analysis of 50 cells (for each respective stress condition and the corresponding time points) was done on Nikon 90i microscope (Nikon Instruments Inc., Tokyo, Japan) using bright field objective at 100× magnification.

2.2.4. Palmelloid formation and dissociation kinetics

For studying the kinetics of palmelloid formation (i.e. association and dissociation), 25 ml of cells cultured as mentioned above was independently grown in TAP media, each containing 100 and 150 mM NaCl for 24 h. For dissociation kinetics, cells grown in TAP medium with NaCl for 18 h were spun at 1100 *g*, for 5 min at 25 °C; washed with 10 ml of TAP medium and re-suspended in fresh TAP medium. At the end of this

experiment, 500 μl from the above samples was harvested at respective time intervals and observed at 40× magnification. The graph is a representation of three independent experiments with biological duplicates within each attempt.

2.2.5. Transmission electron microscopy

The cells were fixed overnight in 2.5% glutaraldehyde in a 100 mM Cacodylate buffer (pH 7.4) at 4 °C, followed by washing twice in the same buffer and then treated with 1% Osmium tetraoxide overnight at 4 °C, dehydrated in an ethanol gradient and treated with 1% Uranyl acetate for 1 h. Samples were then processed through an Araldite-Propylene oxide gradient and finally embedded in Araldite. Thin sections of 70 nm were cut on an ultramicrotome (Leica EM UC7, Leica Microsystems GmbH, Wetzlar, Germany) mounted on grids and observed on a Carl Zeiss Libra 120 TEM (Carl Zeiss AG, Oberkochen, Germany).

2.2.6. Detection, extraction and estimation of starch and neutral lipids

Starch granules were detected by adding one part of Lugol's iodine (6% PI and 4% I_2 crystals) to three parts of fixed cell suspension (untreated and NaCl-treated) and observed under 100× magnification. The protocol for starch extraction was slightly modified from that described by Klein [30]. 25 ml of cells was harvested and re-suspended in 5 ml of ice-cold DDW followed by sonication on ice (Branson Sonifier). Pigments were extracted with 7 ml of acetone and the remaining pellet was washed thrice with 10 ml of ice-cold DDW. Final starch pellet was solubilized in 5 ml of DDW by autoclaving. For starch estimation, 8 μl of iodine solution (0.01% I_2 and 2% PI) was added to 50 μl of the extracted starch samples and incubated at room temperature for 5 min followed by measurement at OD_{600} (Infinite® 200 PRO Nano Quant, Tecan, Männedorf, Switzerland). Lipid staining was carried out as described by Siaut et al., [65] and images were captured with 60× oil immersion objective. Estimation of neutral lipids was carried out as per Kou et al., [31].

2.2.7. Detection and estimation of exopolysaccharides from spent media

Untreated and NaCl-treated cells were stained with ruthenium red (0.1 mg/ml in 1.5 M Tris, pH 8.8) for 10 min at RT followed by microscopic analysis with bright field objective at 100× magnification. Cell-free supernatants were obtained by harvesting the cells at 12,000 *g* for 15 min at 4 °C followed by ~6-fold concentration using a 3 kDa cut-off Amicon Ultra-15 Centrifugal Filter Units (Merck Millipore, India). Hydrolysis of EPSs in supernatants was carried out by boiling 2.5 ml of the concentrates with 1.5 ml of 3 N HCl for 2 h. For estimation, 1 ml of the above hydrolysates was boiled with 2 ml of Anthrone reagent (2% Anthrone in concentrated H_2SO_4) for 10 min; rapidly cooled followed by measurement at OD_{520}.

2.3. Statistical analysis

Wherever quantitative assays were performed, a 2-way ANOVA test with replication was performed and the statistical data are provided as Supplementary tables.

2.3.1. Detection of flagella by immunofluorescence microscopy

Clean cover-slips were coated with 0.1% Polyethyleneimine for 1 h at room temperature followed by washing with DDW and air drying for 30 min. 50 μl of the fixed cells was placed on these cover-slips for 10 min, rinsed briefly with 1× PBS; soaked in methanol for 10 min at −20 °C followed by washing with 1× PBS. The cells were blocked with 3% BSA in 1× PBS for 1 h at RT, washed once with 1× PBS and incubated with Mouse Anti-acetylated tubulin (1:500; Abcam, Cambridge, UK) as above. The cover-slips were washed with PBST (1× PBS with 0.1% Tween 20) and incubated with secondary antibody, Alexa568 conjugated rabbit anti-mouse IgG (1:250; Molecular Probes, Carlsbad, CA, USA) for 1 h at room temperature. After incubation, cover-slips were washed sequentially with PBST, 1× PBS and DDW; mounted on a clean glass slide with Anti-fade reagent (ProLong® Gold, Molecular Probes) and sealed using nail polish. For measurement of swimming speeds, 10 μl of cells was loaded onto a glass cover slip and observed under a 10× objective, affording a large field of view. Each video was converted to individual frames and the distances covered by 30 motile cells (each for control, 100 and 150 mM NaCl stressed samples; after 18 h of stress) was analysed using an image processing software — ImageJ. Self-rotating cells and those that were stuck to the cover-slips were avoided in all the quantifications.

2.3.2. Proteomic analysis of spent media

500 μl of the concentrated cell-free supernatants were dialyzed against 50 mM Tris, pH 7 o/n at 4 °C and processed for SDS-PAGE analysis and silver staining. For iTRAQ analysis, proteins from 400 ml of the cell-free supernatants were precipitated by ammonium sulphate (100% saturation) followed by re-suspension of fractionate in 15 ml of 50 mM Tris, pH 7 and dialysed. Following protein estimation, dialyzed samples were lyophilised (ScanVac, LaboGene, Denmark) and an iTRAQ analysis carried out (Proteomics International, Australia). Briefly, the protein samples were acetone precipitated, reduced, alkylated and trypsin digested according to the iTRAQ protocol (Applied Biosystems). The samples were then labelled using the iTRAQ reagents and pooled. Peptides were desalted on a Strata-X 33 μm polymeric reversed phase column (Phenomenex) and dissolved in a buffer containing 10 mM KH_2PO_4 pH 3 in 10% acetonitrile before separation by strong cation exchange liquid chromatography on an Agilent 1100 HPLC system using a PolySulfoethyl column (4.6 × 100 mm, 5 μm, 300 A). Peptides were eluted with a linear gradient of 0–400 mM KCl. Eight fractions containing the peptides were collected and after desalting on Strata-X columns loaded onto a Agilent Zorbax 300SB-C18, 3.5 μm (Agilent Technologies) running on an Shimadzu Prominence nano HPLC system (Shimadzu). Peptides were resolved with a gradient of 10–40% acetonitrile (0.1% Trifluoroacetic acid) over 160 min. The resultant spots were analysed on a 5600 Triple-TOF mass spectrometer (AB Sciex).

3. Results

To begin with, the effect of several abiotic stressors on the viability of *C. reinhardtii* vegetative cells was assessed using the spot viability assay. This assay offers the advantage of comparing the viability under different conditions; at times, on the same plate involving serial dilution and spotting with a reasonable aliquot of cells. Post exposure to these stress conditions, cells were grown on solid TAP medium and scored for their ability to form colonies. With temperature and alkaline pH stress, viability of cells was unaffected (Fig. S1a, d); and, exposure to acidic pH was detrimental (Fig. S1b). Among osmotic stressors, the effect of NaCl was dose-dependent as exposure to 50–150 mM showed marginal change in viability; while, immediate death was observed with 350 and 500 mM NaCl (Fig. S1c). Cells remained viable in the presence of sucrose in the medium (Fig. S1c); however, addition of 2 mM H_2O_2 affected viability until 1 h after which there was no change in the growth (Fig. S1e). Lower doses of LiCl and Menadione (10 mM and 5 μM, respectively) had no effect on viability; whereas, higher concentrations were detrimental (Fig. S1c, f).

When the morphological effects manifested by stress were scored, heat showed thickening of the starch sheath around the pyrenoids (~45% of the total population) (Fig. S1g), acidic pH induced instant deflagellation accompanied with plasmolysis in all the exposed cells (Fig. S1g). Menadione, H_2O_2 and LiCl showed increased vacuolation and bleaching of chlorophyll (~75% of the total population) (Fig. S1g). As expected, exposure to 10 mM LiCl caused an increase in flagellar length in ~40% of cells after 18 h (Fig. S1g). Instances of increase in cell size ranging from 12 to 15 μm (~15% of the total population) were seen with sucrose. But, 100 and 150 mM NaCl exposure predominantly showed dose- and time-dependent formation of four-celled clusters

(akin to palmelloids) with some instances of cells appearing pigmented (~2%) in these clusters (Fig. S1g).

3.1.1. NaCl stress induced palmelloid formation and dissociation kinetics

A time- and dose-dependent kinetics for the formation of palmelloids was studied using bright-field microscopy. It was found that after 12 h of stress with 100 mM NaCl, palmelloids constituted ~50% of the total cell population which increased to ~80% by the end of 24 h (Fig. 1a, b). The remaining was freely motile vegetative cells. When assayed for extended time points (36 and 48 h), this population distribution attained a plateau (data not shown). Cells treated with 150 mM NaCl followed a similar trend as above Fig. 1a, b.

Incidentally, organic acid-induced palmelloidy in *C. reinhardtii* cells [22] was found to reversible upon transfer of the palmelloids in normal medium [23]. To study the reversible state NaCl-induced palmelloidy, a similar experiment was carried out. Cells were allowed to form palmelloids until 18 h of stress, after which they were washed and re-suspended in fresh NaCl-free TAP medium. The status of cells *vis-à-vis* palmelloidy was monitored microscopically. Surprisingly, all the palmelloids formed in 100 mM NaCl-treated population disappeared within 20 min of de-stress leading to the presence of only unicellular cells (Fig. 2a, b).Motility was also restored in these cells (data not shown). A slightly different trend was observed for palmelloids induced by 150 mM NaCl. The de-stress event was slow as compared to 100 mM NaCl; complete dissociation of palmelloids occurred only after 1 h of de-stress (Fig. 2a, b). In all, 1000 cells were counted per attempt and the corresponding SD values for each time-point are mentioned in the Legends. This event was accompanied with restoration of motility in these cells. Palmelloids induced after 24 h of NaCl stress took ~4 h for complete dissociation while the palmelloidy induced after 36 or 48 h of stress was found to be irreversible accompanied with cell death (data not shown).In order to determine specificity, the palmelloids formed with both 100 and 150 mM NaCl (18 h) were washed and transferred into fresh TAP medium containing the respective concentrations of NaCl. It was observed that the palmelloids were intact under both the treatments (Supplementary Fig. 2).

3.1.2. Ultrastructure studies of palmelloids by TEM

TEM analysis of untreated *C. reinhardtii* cells showed normal morphological features; such as the appearance of a normal cup-shaped chloroplast, nucleus and eyespot (Fig. 3a, b). Palmelloids obtained after 18 h of growth in NaCl-containing medium revealed a common envelope encasing all the cells apart from the individual cell wall (Fig. 3c, d, f, g). With respect to the cell size, two remarkable features

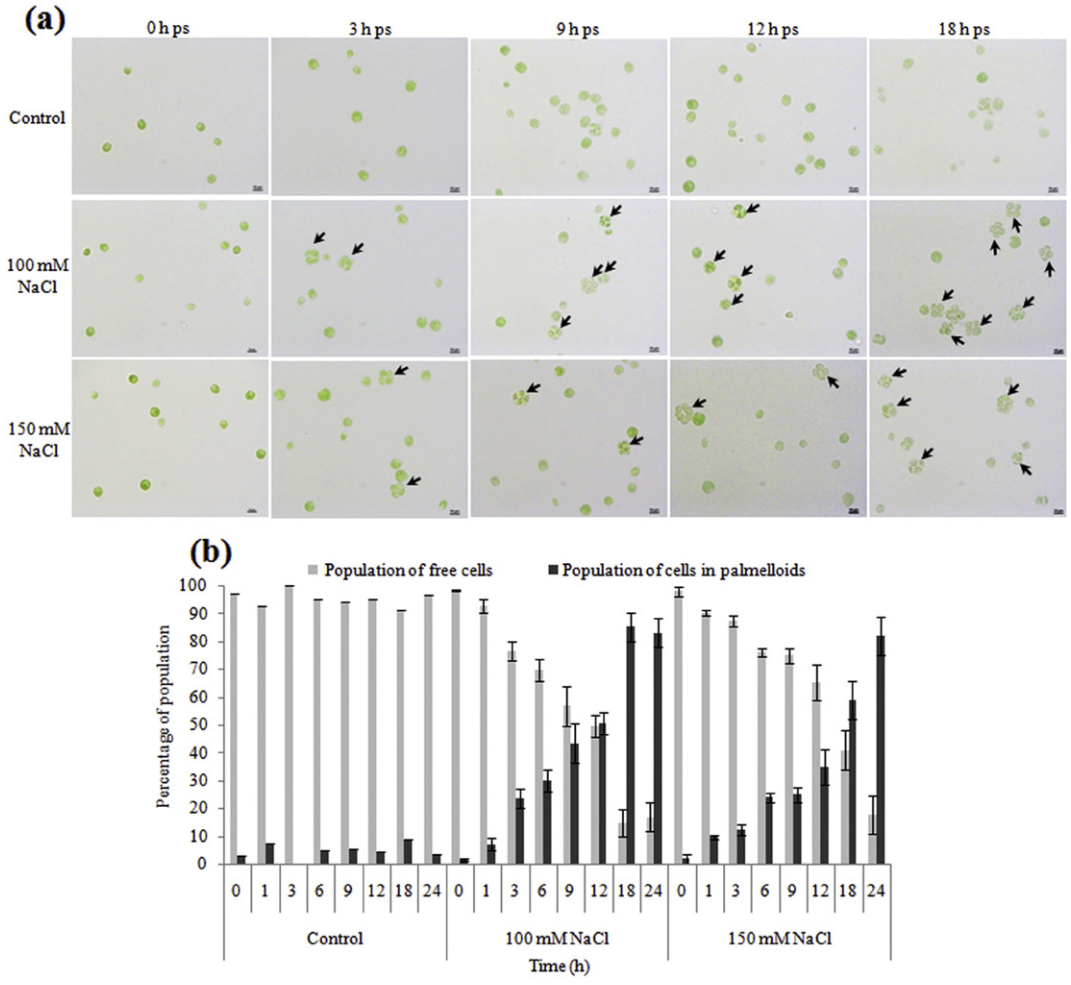

Fig. 1. Kinetics of NaCl stress-inducible palmelloid formation. (a) Qualitative and (b) quantitative analysis of NaCl-induced palmelloid formation. *C. reinhardtii* cells were exposed to NaCl stress and at respective time intervals; aliquots were fixed and analysed microscopically. A dose- and time-dependent increment in palmelloid formation was observed. One thousand cells were counted for every dose and time point in three independent experiments. Error bars show the average of experimental triplicates. Note: ps — post stress. Scale bar corresponds to 10 μm. Using the data from 1(b), a two-way ANOVA test with replication was performed and found to be statistically significant (see Supplementary Tables, T1 and T2).

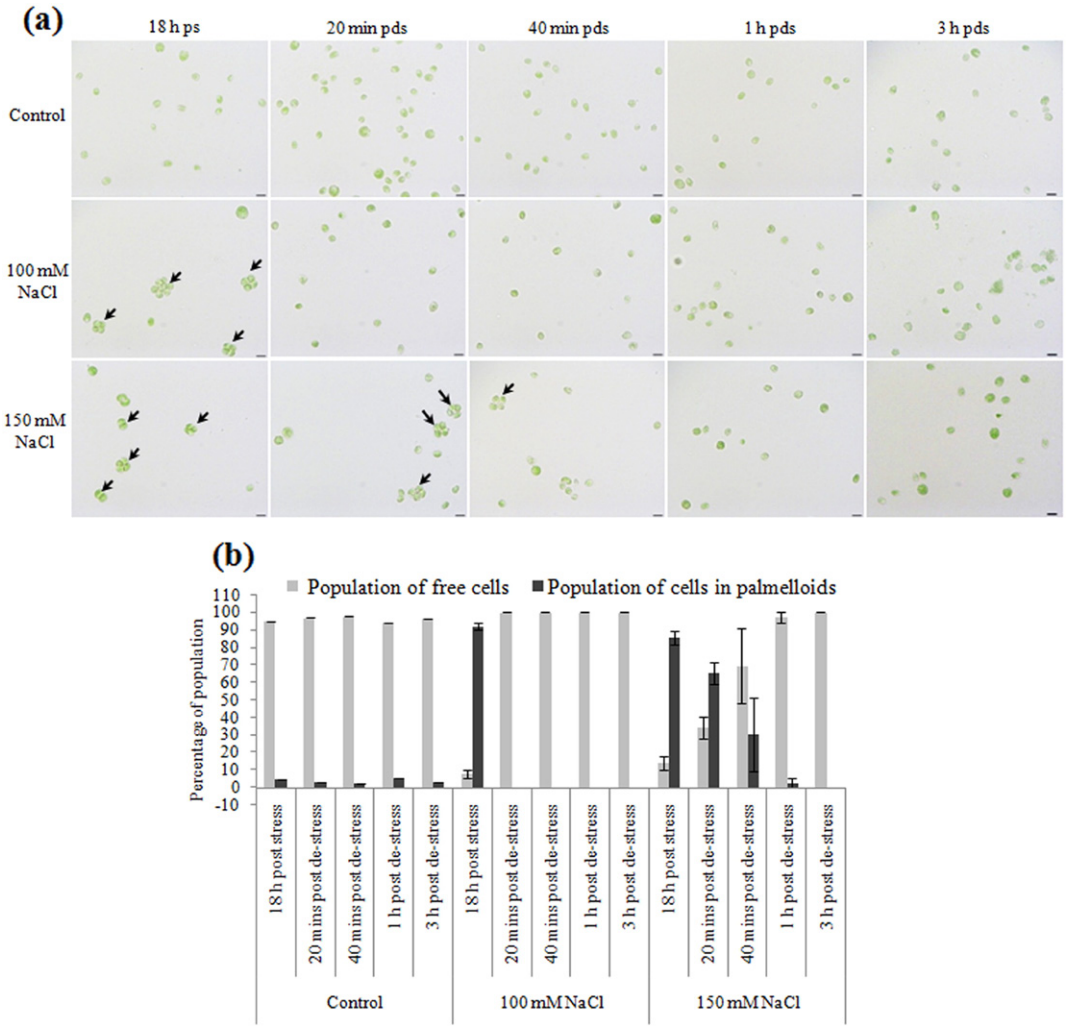

Fig. 2. Dissociation of palmelloids upon NaCl withdrawal. (a) Qualitative and (b) quantitative analysis of palmelloid dissociation. Palmelloids were induced in medium with NaCl for 18 h followed by washing and re-suspension in normal TAP medium. At respective time intervals of de-stress; aliquots were fixed and analysed microscopically. In case of cells treated with 100 mM NaCl, complete dissociation of palmelloid was observed within 20 min of re-suspension in normal medium while for 150 mM NaCl, the dissociation was slow with maximum population of free cells obtained only after 1 h of de-stress. One thousand cells were counted for every dose and time point in three independent experiments. Error bars show the average of experimental triplicates. Note: pds — post de-stress. Scale bar corresponds to 10 μm. Using the data from 2(b), a two-way ANOVA test with replication was performed and found to be statistically significant (see Supplementary Tables, T3 and T4).

were observed. Firstly, there was a reduction in length among these cells; the average cell length in case of 100 mM NaCl treatment was found to be 4.5 μm (SD = ±1.4; n = 45 palmelloids) while for 150 mM NaCl treatment it was 5 μm (SD = ±1.2; n = 35 palmelloids). Secondly, heterogeneity in the sizes among cells within a palmelloid was also consistent (Fig. 3d, f). Another unique feature shown by these cells was the increase in the number and size of the autophagy vacuoles. These structures were found enriched with a lot of electron dense material. Intracellular accumulation of starch and lipid granules was also evident from the TEM analysis. The shape of chloroplasts in these cells was disorganized and the plastids were randomly distributed all over the cells. Flagella with shorter length were present in a few cells. Instances of unidentifiable flagella remnant encased in a vesicle were found in 100 mM NaCl-treated sample (Fig. 3d, discontinuous circle). A flagellar tunnel carrying an electron dense core of the excised transition zone was seen in a palmelloid induced by 150 mM NaCl (Fig. 3f, discontinuous circle). Vesicle-like structures either pinching off from the flagellar membrane (Fig. 3c, zoom in) or clustered around the common wall of the palmelloid (Fig. 3d, zoom in) were also observed. Post 1 h of de-stress, palmelloids dissociated with the release of free cells with normal morphological features (Fig. 3e, h).

3.1.3. Detection of flagella in the palmelloids

While bright-field microscopic analysis revealed the formation of palmelloids, flagella remained undetected, corresponding to our earlier observation that cells within a palmelloid were immotile. In order to confirm this, palmelloids formed after 18 h of NaCl stress were stained with mouse anti-acetylated tubulin followed by probing with Alexa568 conjugated rabbit anti-mouse IgG. Surprisingly, all the cells in the palmelloids showed the presence of flagella albeit of shorter lengths (Fig. 4a). These were measured from captured images using ImageJ software. Palmelloids obtained by 100 mM NaCl showed average flagella length of 4.8 μm (SD = ±1.6; n = 97). A heterogeneity in the palmelloid population w.r.t flagella length was observed in case of 150 mM NaCl; a majority of flagella being too short for measurement while a few (n = 15) showed an average length of 2.5 μm (SD = ±1.3). Also, an accumulation of acetylated tubulin at the tips of the flagella resulting in a bulbous structure was observed in these cases. Motility of free-living cells treated with 50 mM NaCl was similar to that of control cells; while, it reduced by 1.6 to 4-fold in the case of 100 and 150 mM treatments, respectively (Fig. 4b).

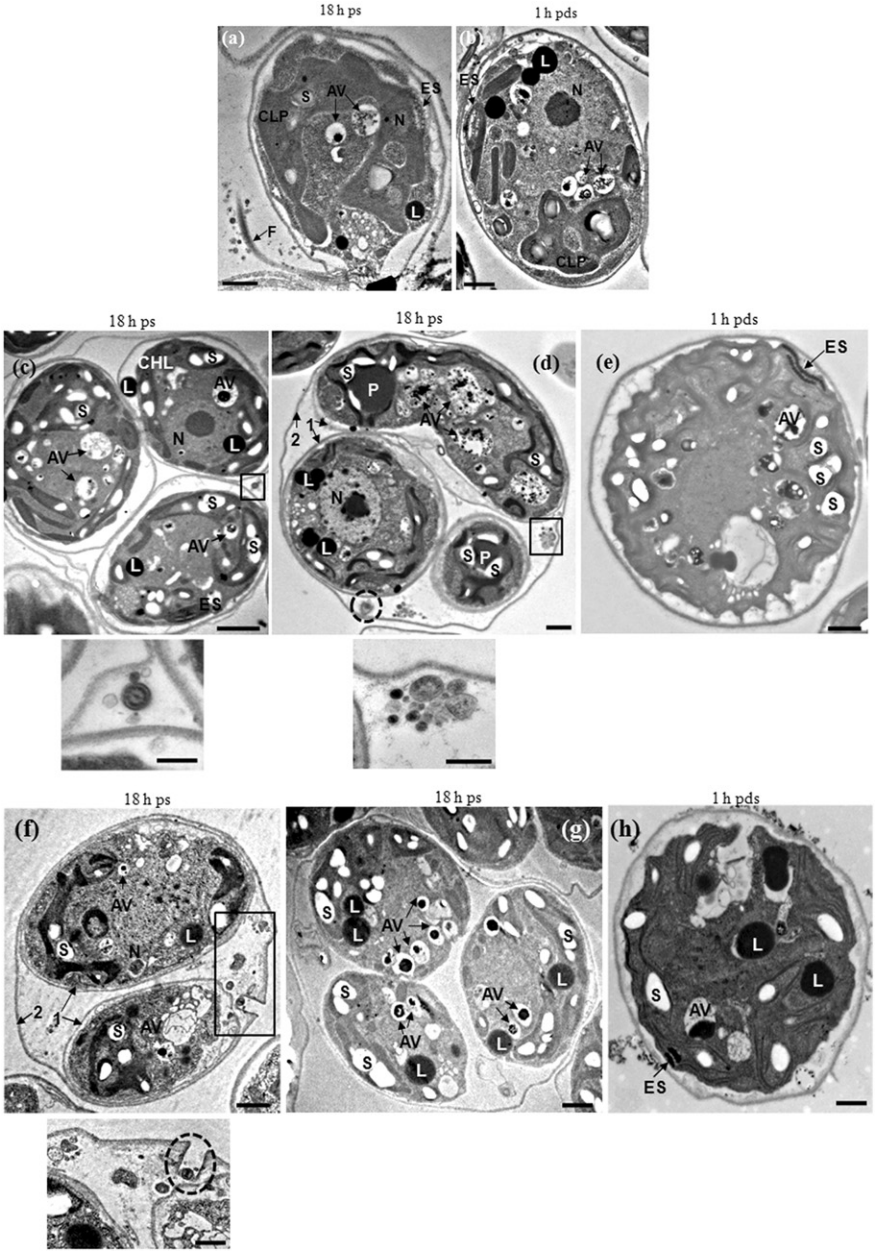

Fig. 3. Ultrastructural studies of palmelloids. (a) and (b) Electron microscopy images of untreated i.e. control *C. reinhardtii* cells. (a) 18 h after growth and (b) 1 h after re-suspension in normal TAP medium. (c–e) Electron microscopy images of *C. reinhardtii* cells treated with 100 mM NaCl. (c) and (d) 18 h post stress; (e) 1 h pds. An overview image is shown above, and a zoom-in of the region demarcated by the black box is shown below. Flagellar tunnel with flagellar remnant (d) is demarcated by discontinuous circle. (f–h) Electron microscopy images of *C. reinhardtii* cells treated with 150 mM NaCl. (f) and (g) 18 h post stress; (h) 1 h pds. Flagellar tunnel with remnant of the transition zone (f) is demarcated by discontinuous circle. Note: CLP, chloroplast; S, starch granule; N, nucleus; ES, eye spot; L, lipid granule; AV, autophagy vacuole; F, flagella; P, pyrenoid; 1, cell wall of the individual cells; 2, common membrane encasing all the cells in the palmelloid. Scale bar in overview images corresponds to 1 μm while those in zoom-ins correspond to 500 nm.

3.1.4. Detection and quantitation of starch, neutral lipids and EPS in palmelloids

TEM analysis revealed that *C. reinhardtii* cells accumulated starch and lipid granules under NaCl stress. Intracellular starch granules were detected using Lugol's iodine. When observed under bright-field objective, ~30% of the cellular area of 18 hps palmelloids appeared bluish–brown in colour (Fig. 5a). Post de-stress, the area occupied by starch granules in free cells diminished within 1 h, with complete absence after 20 h. A quantitative estimation by starch–iodine binding assay (Fig. 5b) revealed that after 12 h of stress, the concentration of the accumulated starch increased two-fold over that of the control (27.8 and 28.9 μg/10^6 cells for 100 and 150 mM NaCl, respectively). This trend continued until 18 h of stress wherein the starch accumulated to 60–68 μg/10^6 cells. Post 20 hpds, the starch concentrations reduced drastically to 11.5–23 μg/10^6 cells.

Neutral lipids accumulated in the stressed cells were detected by a lipophilic stain, Nile red. When observed under a fluorescence objective, neutral lipids appear as granular bodies emitting yellow fluorescence. After 18 hps, a number of such bodies were found in palmelloid cells as opposed to untreated cells where they were absent (Fig. 6a); the numbers for which reduced significantly when free cells were obtained after 1 and 20 hpds. Fluorimetric assay using Nile red was performed to estimate these lipids (Fig. 6b). After 18 hps, the Fluorescence intensity (a.u) was 1.6 fold higher than the respective controls. These values, post 20 hpds, decreased

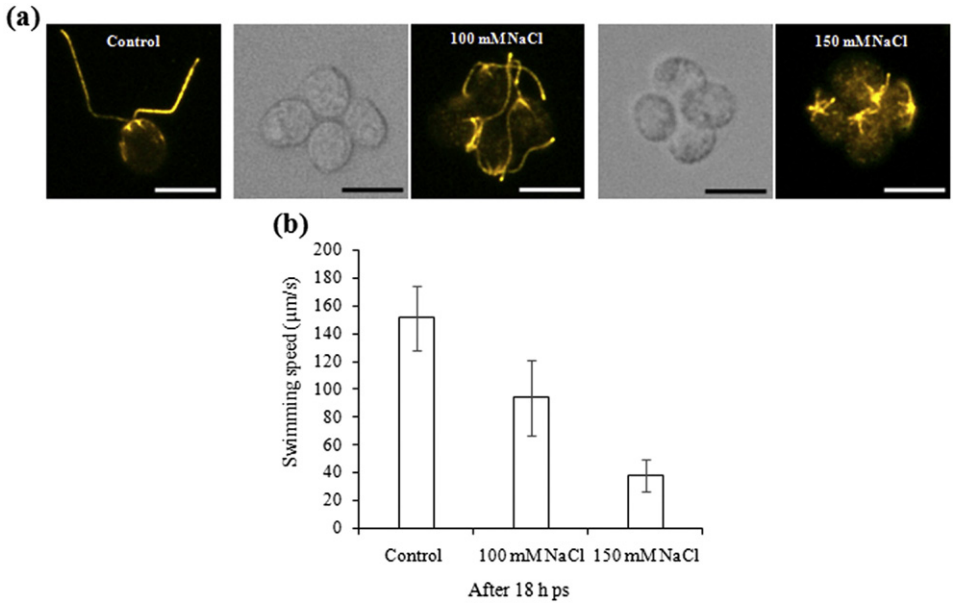

Fig. 4. Detection of flagella in palmelloids. (a) Palmelloids were induced in medium with NaCl and fixed after 18 h of stress. These were stained with primary antibody Mouse Anti-acetylated tubulin followed by staining with secondary antibody Alexa568 conjugated rabbit anti-mouse IgG. The cells were observed with a 60× oil immersion objective under fluorescence microscope. A decrease in the flagella length was observed in cells treated with NaCl. Scale bar corresponds to 10 μm. (b) Videos of unicellular motile cells in the control and NaCl stressed samples (after 18 h ps) were captured under 10× bright field objective and their respective swimming speeds were calculated using Image J software. Error bars show the average of speeds calculated from 30 cells of each sample.

by around 11 and 9.5 fold for 100 and 150 mM NaCl treated cells, respectively as compared to the values obtained 18 hps. This trend indicated a decrease in accumulation of neutral lipids in the cells.

EPSM around the palmelloids was detected using a polysaccharide stain, ruthenium red. After 18 hps, cells were found to be surrounded by EPS (Fig. 7a, arrows). Since only palmelloid cells showed the presence of EPS, quantitative analysis was done for two such time points wherein the population of such cells was maximum in a culture (i. e. after 18 h in NaCl medium) and the other where palmelloids were completely absent in the population (i.e. after 1 hpds). Acid hydrolysis of polysaccharides in the media of these samples resulted in the release of monosaccharide units which were then estimated using the Anthrone reagent (Fig. 7b). A 3.6 fold increase in the EPS concentration after 18 hps and a ~3 fold increase after 1 hpds were estimated in 100 mM NaCl-treated media supernatants as compared to the untreated cells. Similarly, in case of 150 mM NaCl-treated supernatants; ~6 fold increase in the EPS concentration after 18 hps and a 5.4 fold increment after 1 hpds was estimated. Dissociation of palmelloids involves the breaking of extracellular mesh and escape of cells into the favourable environment. This results in the release of EPS into the dissociation medium and hence the presence of EPS is detected even in samples 1 hpds.

3.1.5. Proteomic analysis of the spent medium

In the current study, cells within palmelloids seemed sequestered from a NaCl-rich environment by a common envelope. Thus, the presence of secreted proteins in the culture medium might provide clues about inter-palmelloid communication; if any, as a response against the hostile environment. A steady rise in the number of palmelloids was observed from 3 hps until 18 hps after which a plateau was observed until 24 h. It is speculative for the 18 hps medium to contain proteins that might contribute towards the maintenance of this physiology. One-dimensional SDS-PAGE analysis of the dialyzed and concentrated palmelloid-free spent medium showed a distinct difference in the profile of extracellular proteins; both, after 18 hps and 1 hpds as compared to the respective untreated samples (Fig. S2). Three proteins (*Mr*: 266 ± 26 kDa; 115 ± 1 kDa and 70 ± 1 kDa) were found to be abundant after 18 hps; while, with 1 hpds, eight such proteins with *Mr* ranging from 16 to 274 kDa were identified (arrows, Fig. S2). These results prompted a detailed analysis of these proteins using iTRAQ. In all, two categories of proteins were found to exist. The first category included those that responded to the NaCl stress; while, second belonged to those that responded to the withdrawal of stress (Fig. 8). Both these categories included proteins that were either up-regulated or down-regulated. 41 proteins after 18 hps and 55 proteins after 1 hpds were found to be differentially expressed. Of these, proteins exclusively over-expressed after NaCl stress and down-regulated 1 hpds could be considered to be palmelloid-specific; those abundant only after de-stress could serve to reprogram the palmelloid stage to enter into the 'unicellular' stage; and, might be considered to be vegetative cell-specific (Fig. 8).

Of the 41 proteins identified post 18 hps and when compared with the control, 31 were up-regulated; while, 10 were down-regulated. Among the abundant proteins, five cell wall proteins followed a trend of increased levels with 18 hps that decreased with 1 hpds. Of these, expansin was the most significant (mean fold change ~99) and others such as pherophorins-C5, C6, C9 and hydroxyproline-rich glycoprotein VSP4 showed a mean fold change ranging from 3 to 11 (Table 1). Interestingly, expansin levels were reduced by ~9 fold in the supernatants after 1 hpds. A protein with a WSC domain (cell wall integrity and stress response component protein in yeasts) increased ~6 fold over the control; and again its expression was greatly reduced after de-stress (~0.2 fold) (Table 1). Additionally, three proteins VSP4, pherophorin-C5 (a protein predicted to harbour gametolysin peptidase domain) and a Cathepsin-Z-like protein showed increased levels upon stress exposure; their levels drastically reduced pds. Taken together, expansin, WSC domain protein, pheophorin-C5, VSP4, and Cathepsin-Z-like proteins could all be specific to palmelloid formation. With respect to cellular metabolism, phosphoribulokinase, malate dehydrogenase, serine glyoxylate aminotransferase, 2-enoyl thioester reductase and a predicted Kelch repeat protein with galactose oxidase domain and 6-phosphogluconolactonase-like protein were over-expressed (Table 1). On the contrary, 6-phosphogluconolactonase-like protein was under-expressed by 0.33 fold pds. Surprisingly, ferroxidase (FOX1) involved in cellular iron homeostasis and a protein predicted with hydroxyacyl glutathione reductase domain (implicated in glutathione biosynthetic

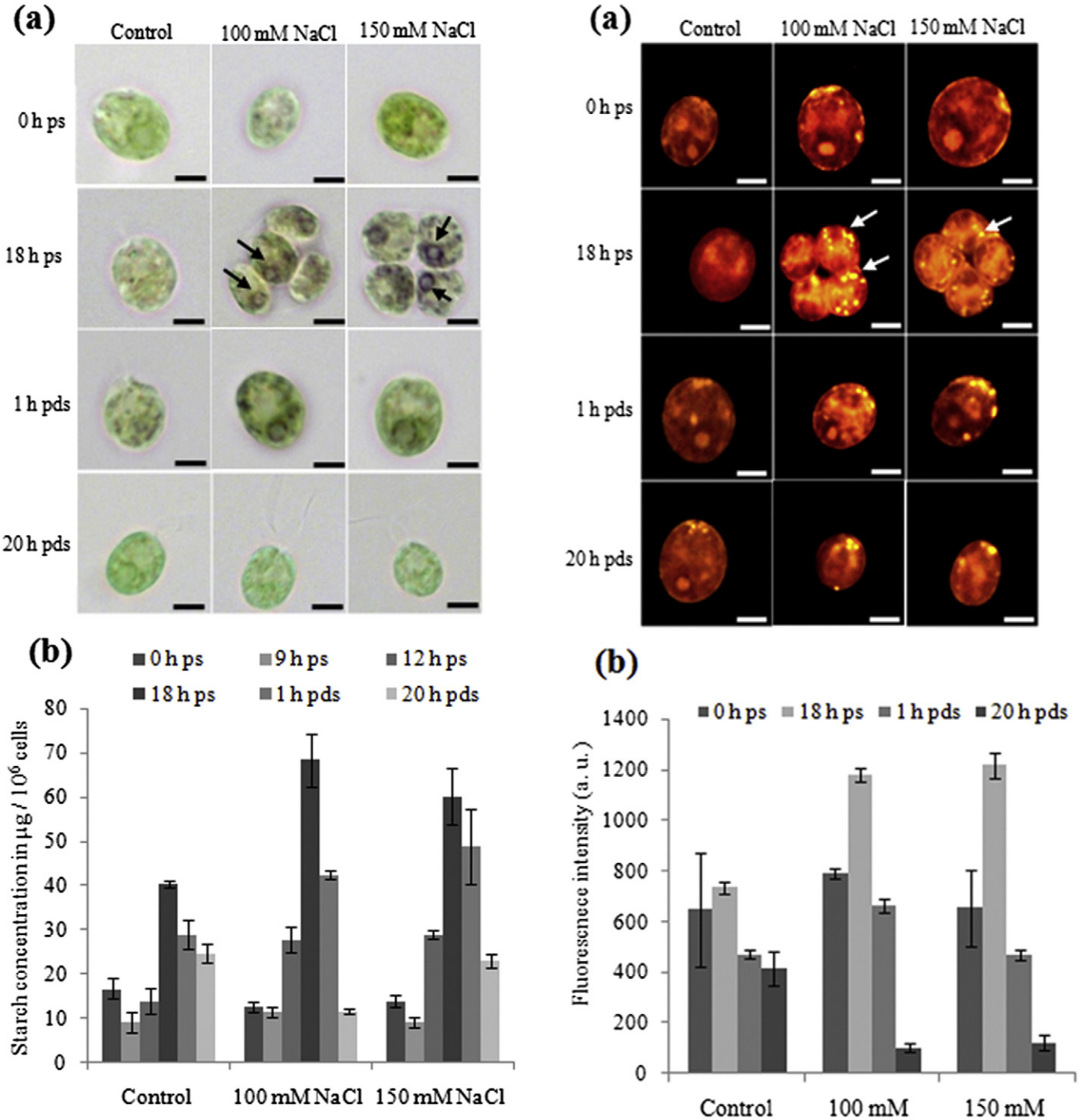

Fig. 5. Accumulation of starch granules in *Chlamydomonas reinhardtii* cells. (a) Qualitative and (b) quantitative analysis of starch granule accumulation. Cells were grown in medium with respective concentrations of NaCl followed by de-stressing in normal TAP medium. Scale bar corresponds to 5 µm. For qualitative assay, accumulated starch granules in palmelloids were stained with iodine solution after 18 h of NaCl stress. The arrows indicate the position of the starch granule in the cell. A decrease in the number of starch granules was observed after 20 h of de-stress. Starch was isolated from cells at respective time intervals and estimated using starch — iodine binding assay. Error bars show the average of three independent experiments. A two-way ANOVA test with replication was performed for the accumulation of starch granules from the data in 5(b) and was found to be statistically significant (see Supplementary Tables, T5 and T6).

Fig. 6. Accumulation of neutral lipids in *Chlamydomonas reinhardtii* cells. (a) Qualitative and (b) quantitative analysis of neutral lipids accumulation. Cells were grown in medium with respective concentrations of NaCl followed by de-stressing in normal TAP medium. Scale bar corresponds to 5 µm. For qualitative assay, neutral lipid granules in palmelloids were stained with a fluorescent lipophilic stain — Nile red after 18 h of NaCl stress. The arrows indicate the droplets of lipid granules accumulated in the cell. A decrease in the number of neutral lipid granules was observed after 20 h of de-stress. Estimation of lipid granules was also done by Nile red fluorescence assay. Error bars show the average of three independent experiments. The quantitative data from 6(b) was used to perform a two-way ANOVA with replication and was found to be statistically significant (see Supplementary Tables, T7 and T8).

pathway) were found to be significantly abundant (mean fold change: 99.1 and 87.9 respectively; Table 1). Also, a noteworthy increment (87.9 fold) in the isoprenyl diphophate synthase concentration indicated isoprene biosynthesis as a response to NaCl stress.

Post 1 h of de-stress, 34 proteins were up-regulated; while, 21 proteins were down-regulated. A protein with PAN/APPLE like domain (mediating protein–protein or protein–carbohydrate interaction) was

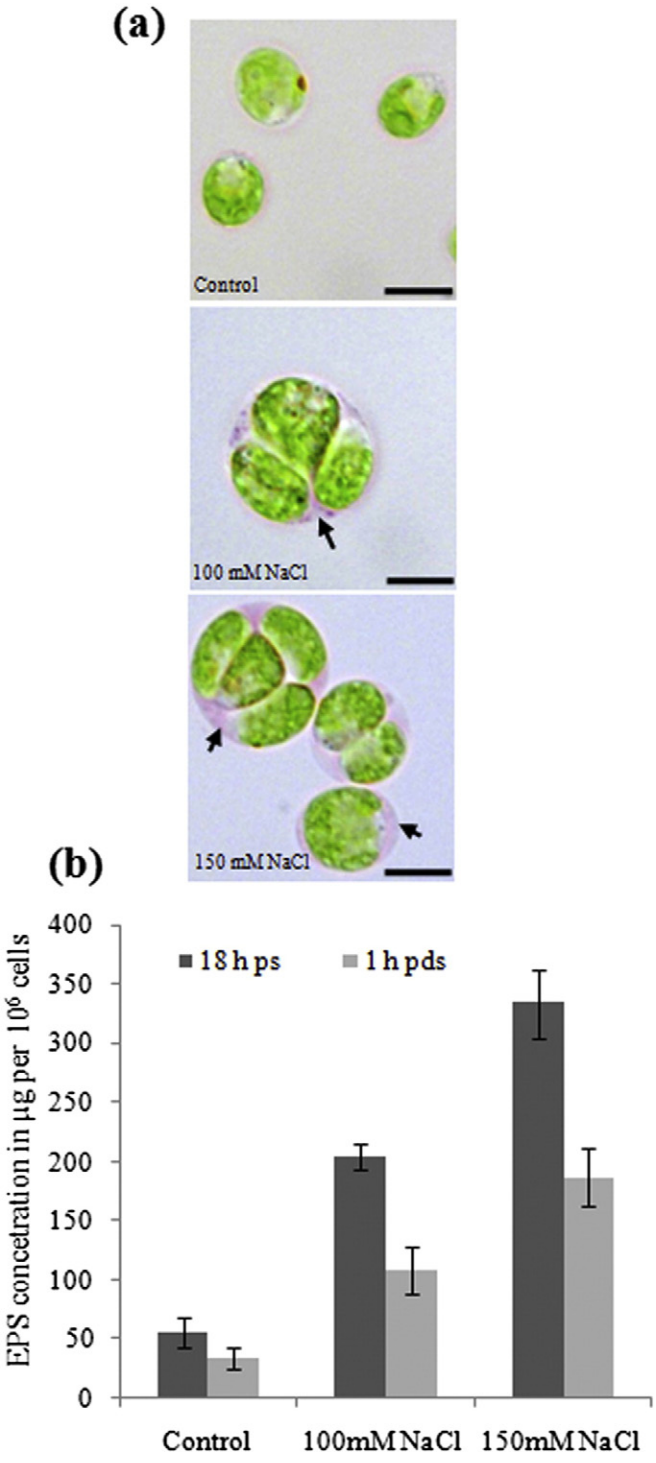

Fig. 7. Detection of EPS *Chlamydomonas reinhardtii* palmelloids. (a) Qualitative and (b) quantitative analysis of EPS. For qualitative assay, EPS surrounding the cells in the palmelloids was stained with a polysaccharide stain — ruthenium red after 18 h of NaCl stress. Scale bar corresponds to 10 µm. The arrows indicate the accumulation of EPS around the cell. EPS was purified at respective time intervals and quantified by Anthrone assay. Error bars show the average of three independent experiments. The data from 7(b) was used to perform a two-way ANOVA with replication and was found to be statistically significant (see Supplementary Tables, T9 and T10).

found to be the most abundant (mean fold change: 99.1); while, its level was only ~7 fold higher after NaCl exposure representing its negative role in palmelloidy (Table 1). Further, cell wall glycoprotein GP2 and a matrix metalloproteinase MMP13 were found to be strongly up-regulated pds; while, they were severely down-

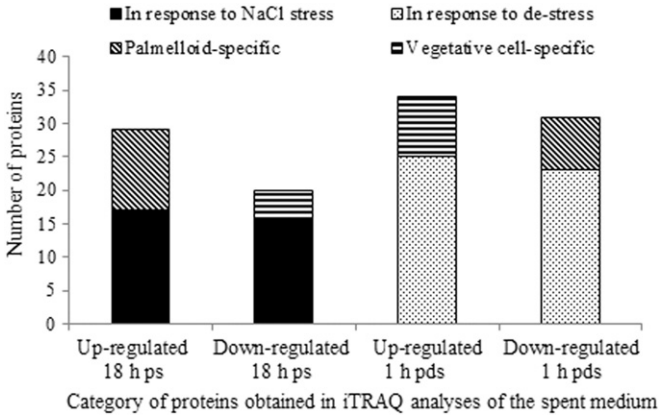

Fig. 8. Distribution of proteins in control, NaCl-exposed and de-stressed spent media. The number of proteins up-regulated and down-regulated 18 hps and 1 hpds were plotted taking into account the p value as ≤0.005, resulting in two distinct categories, palmelloid-specific proteins and vegetative cell-specific.

regulated post NaCl exposure (Table 1). Other proteins such as matrix metalloproteinase MMP3, cell wall glycoprotein GP3, pherophorins-C15 and -C17, hydroxyproline-rich cell wall protein ISG were exclusively up-regulated during de-stress exhibiting the probable alterations in cell wall composition (Table 2). A soluble inorganic pyrophosphatase was found to be up-regulated by ~99 fold while another protein sharing homology with aspartate aminotransferases from other organisms and a predicted protein (*Mr* ~ 50 kDa) were also found to be 87-fold abundant pds conditions (Table 2). These proteins might play a role in resurrecting the cells from the palmelloid physiology. Two flagellar proteins namely flagellar associated protein FAP174 and intraflagellar transport protein 144 was also significantly up-regulated (~88- and ~57-fold respectively) only after de-stress condition (Table 2). A noteworthy abundance (~88-fold) of two predicted proteins homologous to 2-enoyl thioester reductases and dehydrogenases from other organisms was also restricted to de-stress regime. Surprisingly, Fe-assimilating protein 1(FEA1/H43) was also up-regulated (19-fold) 1 hpds (Table 2).

Proteins found to be under-expressed in both stress as well as de-stress scenarios were phosphoserine aminotransferase, thioredoxin, acyl carrier protein and calcium sensing receptor (Table 1). Proteins such as flagellar membrane glycoprotein 1B, autolysin and phosphoglucomutase GPM1a were exclusively under-expressed post stress (Table 2). Other proteins down-regulated after 1 hpds with a fold change above 0.5 were ODA5 associated flagellaradenylate kinase (FAK1), Ribose-5-phosphate isomerise (RPI1) and Glycine cleavage system, P protein (GCSP) (Table 2). In addition to the aforementioned, many other proteins were also differentially expressed but their fold changes were less than 10 for up-regulation and 0.5 for down-regulation. These have been summarized in Tables 1–2.

4. Discussion

4.1. Stress-inducible responses in C. reinhardtii

Several studies using *C. reinhardtii* involved direct exposure of vegetative cells to effective doses of stress agents such as UV-C [44], acetic acid [84], Mastoparan [83], low temperature [73], NaCl [51,67], Menadione [68] and H_2O_2 [67]; thus providing an insight on the short-term stress responses. In another approach, cells were first allowed to acclimatize to sub-lethal doses of the stress agent for a stipulated time followed by exposing the survivors to higher than sub-lethal doses [19,47]. This aided in understanding the probable long-term defence mechanisms adopted by this organism towards stress tolerance.

In the present study, the former approach was adopted with assessment of the cell viability and morphology being used as a primary screen

Table 1
Proteins differentially expressed both under stress and de-stress conditions. The proteins from the control, stress and de-stress spent media were analysed using iTRAQ. Spectral data were analysed against the UniProt *C. reinhardtii* database using ProteinPilot™ 4.5 Software (AB Sciex). This list was generated after applying a p-value filter ($p \leq 0.05$). ↑ Indicates up-regulated proteins and ↓ indicates down-regulated proteins. Homology and domain searches for the proteins were performed by NCBI BLAST (http://blast.ncbi.nlm.nih.gov/Blast.cgi) and NCBI-Special BLAST-Conserved Domains (http://www.ncbi.nlm.nih.gov/cdd) respectively; while, they were assigned pathways according to KEGG pathway tools (http://www.genome.jp/kegg/pathway.html).

Sr no.	Uniprot accession no.	Protein name	NaCl: control	PVal	NaCl: control	PVal	Domain/Pathway involved/Function	Subcellular location
			After 18 of stress		After 1 h of de-stress			
1.	A8IDR1	Expansin	99.1↑	0.0178	11.7↑	0.033	Cause pH induced cell wall extension in plant cells	Cell wall
2.	A8HTY0	Plastid ribosomal protein L7/L12	8.6↑	0.0027	0.03↓	0.0035	Structural constituent of ribosome	Chloroplast/nucleus/cytoplasm
3.	A8J1H4	Predicted protein	7.9↑	0.0353	99.1↑	0.0178	Has PAN/APPLE like domain. Mediate protein–protein or protein-carbohydrate interaction	Not predicted
4.	A8HNS2	Predicted protein (Fragment)	7.1↑	0.0266	0.6↓	0.015	Gametolysin peptidase M11. Cell wall degradation	Extracellular matrix
5.	A8HQW1	6-phosphogluconolactonase-like protein (Fragment)	6.7↑	0.0017	0.3↓	0.0138	Pentose phosphate shunt	Chloroplast
6.	A8IR73	Predicted protein	5.8↑	0.0016	0.2↓	0.0026	Has WSC domain involved in carbohydrate binding. In yeast it maintains cell wall and is a stress response protein	Cell wall
7.	A8INZ2	Cell wall protein pherophorin-C9 (Fragment)	5.0↑	0.001	6.↑	0.0056	Carbohydrate binding and cross-linking in cell wall	Cell wall
8.	A8IA98	Predicted protein	4.9↑	0.0312	1.4↑	0.034	Has pherophorin domain	Not predicted
9.	Q3HTK2	Pherophorin-C5 protein	3.2↑	0.0033	0.2↓	0.0101	Carbohydrate binding and cross-linking in cell wall	Cell wall
10.	A8JGJ0	Predicted protein	3.0↑	0.0172	0.1↓	0.0354	Cathepsin Z like protein. Acts as a carboxypeptidase	Not predicted
11.	A8IRQ1	Ribose-5-phosphate isomerase	2.7↑	0.0009	0.7↓	0.0096	Pentose phosphate shunt	Chloroplast
12.	Q94C44	Hydroxyproline-rich glycoprotein VSP4	2.6↑	0.0024	0.1↓	0.0298	Cell wall component	Cell wall
13.	A8ITZ2	Predicted protein (Fragment)	2.5↑	0.0178	39.1↑	0.0158	Partial homology with glycine dehydrogenase	Not predicted
14.	Q6PLP6	Cell wall protein GP2 (Fragment)	0.4↓	0.0301	32.5↑	0.0061	Cell wall formation	Cell wall
15.	A8JDG4	Monodehydroascorbatereductase	0.2↓	0.04	1.9↑	0.0392	Oxidoreductase participating in the ascorbate - glutathione pathway for detoxification of ROS	Chloroplast, cytoplasm, mitochondria
16.	A8J363	Matrix metalloproteinase-like protein MMP13	0.2↓	0.0157	10.9↑	0.003	Endopeptidase activity	Extracellular matrix
17.	Q1RS83	Pyruvate formate-lyase	0.1↓	0.007	1.8↑	0.0018	Anaerobic glucose metabolism	Cytoplasm

to gain a comprehensive understanding of the responses elicited in *C. reinhardtii* cells upon independent exposure to an array of abiotic stress agents. The response of vegetative cells w.r.t viability and morphological changes varied. By and large, growth and morphology remained unaffected when exposed to medium with alkaline pH medium or when incubated at low temperatures (7 °C and 15 °C) (Fig. S1a, d).With exposure to low pH or Mastoparan, instant deflagellation via G-protein mediated activation of Phospholipase C [59] has been observed earlier. Along with the deflagellation, the present study also showed plasmolysis leading to rapid cell death in the acidic pH medium (Fig. S1b, g). *C. reinhardtii* cells showed a significant reduction in recovery growth post 2 h exposure to high temperatures i.e. 40 °C and 42 °C [19]. On the contrary, when cells were incubated at 40 °C, no such effect on growth was observed until 3 h of incubation in the current study (Fig. S1a). Also, thickening of the starch sheath around the pyrenoids was observed in case of heat stress (Fig. S1g). Interestingly, recent report of *C. reinhardtii* CC-503 cells cultured at 5 °C has shown a similar morphological change [73]. Another study showed that acclimatized *C. reinhardtii* cells showed severe reduction in growth when challenged with concentrations higher than 150 mM NaCl/10 mM LiCl/10 μM Menadione [19]. In the present study, similar response with non-acclimatized cells was obtained with NaCl, LiCl and Menadione stress (Fig. S1c, f). Additionally, 10 mM LiCl in the medium caused an increase in flagellar length as reported earlier ([50]; Fig. S1g). Incorporation of 2 mM H_2O_2 in the medium had marginal effect on cell viability until 1 h, after which the cells grew similar to the untreated cells (Fig. S1e). Under dark conditions, 2 mM H_2O_2 added in the medium degrades by 50% within 1 h of incubation followed by complete disappearance from the medium by 4 h [64]; thus explaining the early effect of H_2O_2 on cell viability. Additionally, earlier work in the laboratory showed that 10 mM H_2O_2 induces PCD in the vegetative cells of this alga [67]. The physiological changes manifested by all the oxidative stress agents were however similar (Fig. S1g). Medium supplemented with sucrose had no effect on cell growth, but, an increase in cell size was seen (Fig. S1c, g).

Curiously, when exposed to 100 or 150 mM NaCl, formation of four-celled clusters was predominant accompanied with a loss in motility (Fig. S1g). The cell size in these clusters was reduced by half of the untreated cells. A steady increase in the cluster population was observed till 18 h of NaCl stress after which it attained a plateau. We believe that these clusters are palmelloids and a detailed overview *vis-à-vis* our finding follows.

4.2. NaCl-induced palmelloids and their characteristic features

C. reinhardtii typically grows in 2^n cell volume before a rapid succession of *n* rounds of mitosis usually with $n = 2$ (sometimes 3), but not more than 5. Before mitosis ensues, flagella are resorbed and the cell becomes immotile. Cell wall formation ends the process of mitosis; cells are separated and the flagella regrow to their normal length, the mother sac is dissolved and daughter cells hatch out. Usually free-swimming in liquid media, *C. reinhardtii* cells become non-flagellated on solid substrate, upon immobilization. Like many other green algae, *C. reinhardtii* also exhibit a phenotype when stressed — cells fail to separate/get released from the mother sac cell wall after *n* rounds of mitosis. This leads to an apparent aggregation or flocculation of cells as tetrads, octads, or even larger clumps of 2^n cells. When grown on agar, these aggregated cells form colonies that are 'soupy' or gelatinous as a result of releasing acidic polysaccharide mucilage—and exhibit morphological identity to palmelloids, seen for the algae *Palmella* and *Gloeocystis* in the order *Tetrasporales* [18]. The palmelloid condition is often accompanied by the production of gelatinous extracellular material consisting mainly of acidic polysaccharides (which has been used as a soil conditioner in *Chlamydomonas mexicana*) [12]. This mucilage is rich in hydroxyproline-containing glycoproteins similar to the cell wall [35, 42] and the ECM of other colonial Volvocaleans like Volvox. In this phenotype, cells do not 'hatch' properly after cell division and therefore, adhere to one another forming clusters. Clusters of four to eight cells encased in common walls, and aggregates of four-celled groups adhere

Table 2
Proteins unique to the spent media from the stress or de-stress regimes. The secreted proteins from the control, stress and de-stress spent media were analysed using iTRAQ. Spectral data were analysed against the UniProt *C.reinhardtii* database using ProteinPilot™ 4.5 Software (AB Sciex). This list was generated after applying a p-value filter ($p \leq 0.05$). Homology and domain searches for the proteins were performed by NCBI BLAST (http://blast.ncbi.nlm.nih.gov/Blast.cgi) and NCBI-Special BLAST-Conserved Domains (http://www.ncbi.nlm.nih.gov/cdd) respectively while they were assigned pathways according to KEGG pathway tools (http://www.genome.jp/kegg/pathway.html).

Sr no.	Uniprot accession no.	Protein name	NaCl: control	PVal	Domain/Pathway involved/function	Subcellular location
Proteins up-regulated only after 18 h of NaCl stress						
1	Q8LL91	Ferroxidase-like protein (FOX1)	99.1	0.0178	Cellular iron ion homeostasis	Cell membrane
2	A8HX52	Predicted protein	87.9	0.0174	Has IsoprenylDiphosphate Synthase domain involved in isoprene biosynthesis	Not predicted
3	A8JHU0	Malate dehydrogenase (MDH4)	87.9	0.0177	TCA cycle	Chloroplast/cell wall/membrane
4	A8ISA8	Predicted protein	87.9	0.0186	Homology with Kelch repeat proteins. Has a galactose oxidase central domain	Not predicted
5	A8JGY2	Predicted protein	87.9	0.0185	Homology with hydroxyacylglutathionereductase proteins. Has a hydroxyacylglutathione hydrolase (glyoxalase 2) domain catalysing removal of toxic compound methylglyoxal. Involved in glutathione biosynthetic pathway	Not predicted
6	A8IYP4	Phosphoribulokinase (PRK1)	87.1	0.0197	Calvin cycle	Chloroplast
7	A8HNR9	Predicted protein	11.9	0.0276	Hypothetical protein. No putative conserved domains detected	Not predicted
8	Q3HTK1	Pherophorin-C6 protein	10.8	0.0178	Carbohydrate binding and cross-linking in cell wall	Extracellular matrix
9	A8I4Q2	Predicted protein	9.5	0.0182	Shares homology with FAP 211 & FAP212 from *C. reinhardtii*. These proteins were found to be secreted even during CO_2 stress	Not predicted
10	A8JFZ0	Serine glyoxylate aminotransferase (SGA1a)	8.3	0.0167	Amino acid metabolism	Not predicted
11	A8J7S1	Predicted protein	6.7	0.0019	Shares some homology with a envelope glycoprotein from HIV-1. No putative conserved domains detected	Not predicted
12	A8HUE0	Eukaryotic translation initiation factor 6 (EIF6A)	6.5	0.0191	Binds to the 60S ribosomal subunit and prevents its association with the 40S ribosomal subunit to form the 80S initiation complex in the cytoplasm	Cytoplasm/nucleus
13	A8IYP5	Thioredoxin h2 (TRXh2c)	4.5	0.0284	Cell redox homeostasis	
14	A8J3Y6	AIR synthase-related protein	4.2	0.0386	Involved in purine biosynthesis	Plastids/mitochondria
15	A8JF18	Ubiquitin, minor isoform (UBQ1a)	2.3	0.0241	Ubiquitination	Not predicted
16	A6Q0K5	Calvin cycle protein CP12, chloroplastic (CP12)	1.6	0.0329	Calvin cycle	Chloroplast
17	A8IKW6	Ribulose-phosphate 3-epimerase (RPE1)	1.4	0.0034	Calvin cycle/Pentose phosphate pathway	Chloroplast
Proteins down-regulated only after 18 h of NaCl stress						
1	P31178	Autolysin	0.9	0.0452	Cell wall biogenesis/degradation	Cell wall/extracellular matrix
2	A8I341	Predicted protein	0.9	0.0398	Has a phospholipase B domain	Not predicted
3	Q84X68	Flagella membrane glycoprotein 1B	0.9	0.0187	Necessary for gliding motility	Flagella membrane
4	A8HQK6	Predicted protein (fragment)	0.3	0.031	Has a Laccase-like multicopper oxidase domain	Not predicted
5	A8IAN1	Transketolase	0.2	0.0015	Transketolase activity	Chloroplast envelope
6	A8J728	Predicted protein	0.2	0.0152	This protein has a polyketidecyclaseSnoaL-like domain	Not predicted
7	A8J1C1	Ubiquitin-activating enzyme E1 (UBA1)	0.1	0.0042	ATP binding; Ubiquitin-protein transferase activity	Cytoplasm/cell membrane
Proteins up-regulated only after 1 h of de-stress						
1	A8J133	Soluble inorganic pyrophosphatase (IPY3)	99.1	0.0189	Inorganic diphosphatase activity. Might participate in lipid storage or metabolism of phosphate-containing compounds	Cyotsol/nucleus
2	A8I6B9	Predicted protein	87.9	0.0171	Homologous to dehydrogenases from other organisms. Has a Rossmann-fold NAD(P)H/NAD(P)(+) binding (NADB) domain.	Not predicted
3	A8HQU6	Predicted protein	87.9	0.0166	Homology with Aspartate aminotrasnferases from other organisms	Not predicted
4	A8IUS4	Predicted protein	87.9	0.0181	Predicted protein only from *Chlamydomonas*	Not predicted
5	A8I439	Flagellar associated protein (FAP174)	87.9	0.0172	Not predicted	Flagella
6	A9XPA7	Intraflagellar transport protein 144 (IFT144)	56.5	0.0203	Participates in intracellular protein transport or vesicle mediated transport	Membrane coat or flagella
7	A1IVY2	Cell wall glycoprotein GP3	25.8	0.0045	Cell wall formation	Cell wall
8	A8IWE4	Predicted protein (fragment)	21.1	0.017	Homologous to extracellular matrix glycoprotein pherophorin-V29 (Volvox)	Not predicted
9	Q9LD42	Fe-assimilating protein 1 (h43)	16.6	0.0193	High CO_2 inducible protein	Periplasm
10	A8J879	Cell wall protein pherophorin-C17 (PHC17)	12.1	0.0316	Carbohydrate binding and cross-linking in cell wall	Extracellular matrix

Table 2 (*continued*)

Sr no.	Uniprot accession no.	Protein name	NaCl: control	PVal	Domain/Pathway involved/function	Subcellular location
11	A8JAQ5	Flagellar associated protein (ANK17)	10.8	0.0156		Flagella
12	A8I9N1	Predicted protein (fragment)	9.5	0.0178	Homologous to importin or karyopherin alpha subunits from other organisms. Has two Armadillo/beta-catenin-like repeats involved in protein–protein interactions	Not predicted
13	A8JBJ1	Hydroxyproline-rich cell wall protein (fragment) (ISG-C4)	7.4	0.002	Cell wall component	Cell wall
14	A8IZV1	Matrix metalloproteinase (MMP3)	6.6	0.0132	Endopeptidase activity	Extracellular matrix
15	A8HP90	Ribosomal protein L6 (RPL6)	6.6	0.0176	Translation	Chloroplast/nucleus/ribosome/cytosol
16	A8J926	Fasciclin-like protein (FAS7)	6.4	0.0374	Cell adhesion	Cell wall
17	Q27YU0	Radial spoke protein (RSP1)	6.4	0.018		
18	A8IT00	Carbonic anhydrase, alpha type, periplasmic (CAH2)	3.9	0.0023	Catalyse reversible interconversion of carbondioxide and carbonate	Periplasm
19	A8HM32	Predicted protein (fragment)	3.3	0.0321	Has homology with mitochondrial-like trans-2-enoyl-CoA reductase. Harbours a 2-enoyl thioesterreductase (ETR) domain involved in fatty acid synthesis	Not predicted
20	A8IZY9	Cell wall protein pherophorin-C15	3.2	0.0348	Carbohydrate binding and cross-linking in cell wall	Extracellular matrix
21	A8HSS0	Oligopeptidase A (THO3)	3.1	0.0171	Metalloendopeptidase activity	Cytosol/chloroplast stroma
22	A8I9J4	Nucleoredoxin 2 (NRX2)	2.7	0.0319	Cell redox homeostasis	Nucleus/Cytoplasm
23	A8JFZ4	Predicted protein	2.4	0.0356	Has homology with dimethylallyltransferase. Harbours a glutamine amidotransferase (GATase1)-like domain	Not predicted
24	A8ICW5	Predicted protein	2.4	0.032	Has a SAM (Sterile Alpha Motif) domain. These proteins interact with other proteins, RNA & lipids. They also participate in signal transduction & RNA transcription	Not predicted
25	A8IMD2	Predicted protein (fragment)	1.9	0.0099	Has Grip and coiled-coiled domain used in targeting.	Not predicted
Proteins down-regulated only after 1 h of de-stress						
1	A8HQF3	ODA5-associated flagellaradenylate kinase (FAK1)	0.9	0.0376	Belongs to Adenylate kinase family	Flagella
2	A8IVM9	Glycine cleavage system, P protein (GCSP)	0.6	0.0495	Glycine dehydrogenase activity. Involved in glycine catabolsim	Chloroplast
3	A8J9X1	Mitochondrial F1F0 ATP synthase, delta subunit ATP4	0.5	0.0497	ATP synthesis	Mitochondria
4	A8JG58	Predicted protein	0.3	0.0097	Has a Glycyl-tRNAsynthetase (GlyRS)-like class II core catalytic domain	Cytosol, endosome or trans-golgi network
5	A8HMQ1	Aconitatehydratase (ACH1)	0.3	0.0321	Enzyme related to TCA cycle	Chloroplast/Mitochondria
6	A2PZC2	UDP-Glucose: proteintransglucosylase (EZY11)	0.2	0.0267	Cellulose biosynthetic pathway	Cell wall/Golgi cisternae/vacuolar membrane
7	A8HY43	Thylakoid lumenal protein (TEF14)	0.2	0.0476	Thylakoid biogenesis	Chloroplast
8	A8I1X7	Predicted protein (fragment)	0.2	0.0478	Has a Scavenger receptor cysteine-rich domain. These are extracellular domains involved in protein–protein interactions	Membrane protein
9	A8J135	Predicted protein	0.2	0.0426	Has some homology with membrane protein from soil bacterium	Not predicted
10	A8JC04	Phosphoglycerate kinase (PGK1)	0.2	0.0001	Enzyme related to glycolysis	Cytoplasm, chloroplast or mitochondria
11	A8J8Z2	Phosphoglucomutase (GPM1a)	0.2	0.0124	Starch biosynthesis pathway	Chloroplast or chloroplast envelope
12	Q45QX6	Central apparatus associated protein C1a	0.2	0.0491	Not predicted	Flagella
13	A8IFC8	Selenium binding protein (SBD1)	0.1	0.0286	Selenium binding protein	Cytosol

to one another. The individual cells appear normal in structure and in some cases even have very short (but structurally normal) flagella [50]. The palmelloid condition, at least in these cases, is due to a failure of hatching or release from the mother sac (sporangia) and does not result from aggregation of previously swimming cells.

Palmelloids are not primarily due to the aggregation of free-swimming, non-clonal cells. They are now known to be formed by *Chlamydomonas* cells under different conditions of stress like decrease in calcium concentration below 0.1 mM, organic acids [22], chloroplatinic acid [49], phosphate limitation [53], acidic environment [76], rotifer [38] and herbicide paraquat [24]. All these studies described certain characteristic features associated with palmelloid formation such as EPS secretion, clustering of cells with varying number (minimum being a two-celled cluster), cells embedded in the EPSM surrounded by a common envelope,

individual cell wall thickening, abnormal cell division, and reduced individual cell size. In the current study, four-celled palmelloids were predominant that persisted even after 36–48 h of incubation for in NaCl-containing medium (data not shown). Viability of NaCl-induced palmelloids was also compromised after 48 h unlike in *C. eugametos* [49] and *C. applanata* [76] where the palmelloids could survive for five days. Interestingly, low pH-induced palmelloids of *C. applanata* formed cellular clumps that were visible to the naked eye [76].Similar findings were reported in a recent study by Neelam and Subramanyam [51]. In fact, it is known that some algal species form 'akinetes' or asexual resting spores in which a vegetative cell thickens its cell wall and accumulates carotenoids, starch, and lipids in preparation for harsh conditions [9]. We hypothesise that the palmelloid state may be an akinete state that may enable asexual cells to survive periods of chronic stress such as NaCl salt (current study) or starvation under conditions where zygospore formation is not possible (i.e., under conditions where nitrogen is not limiting).

TEM analysis of *C. eugametos* palmelloids [49] showed that though the flagella had no abnormalities at the ultrastructural level, cell motility was inhibited [49]. *C. applanata* palmelloids were reported to have severed flagella thus compromising motility in these cells [76]. When exposed to the rotifer *B. calyciflorus*, *C. reinhardtii* cells lost flagella and formed palmelloids as a strategy to escape grazing by increasing the particle size [38]. In the present study, cells in the NaCl-induced palmelloids were non-motile and may have either lost or paralysed their flagella. Immunofluorescence microscopy using Anti-acetylated tubulin antibody showed the presence of flagella in these palmelloids; but their lengths were reduced to half in case of palmelloids formed with 100 mM NaCl and to one-fourth in those exposed to 150 mM NaCl (Fig. 4). Upon de-stress, palmelloids formed with 150 mM NaCl took ~1 h to revert to the unicellular, motile state; while, those formed in 100 mM NaCl reverted within 20 min of de-stress. Excision of flagella followed by delivery of excised flagella and transition zone remnants in the extracellular environment is a requisite event before the cell undergoes mitotic division. This process follows a specific pathway wherein the remnants are encased in vesicles and delivered into the surrounding environment via the formation of specialized structures named flagellar tunnels [55]. Such structures were observed in the NaCl-induced palmelloids suggesting that the cells underwent mitotic division (Fig.3d, f, discontinuous circles). A recent study by Wood and co-workers [79] puts forward a novel finding that the vegetative lytic enzyme (VLE) necessary for degradation of mother cell wall and release of newly formed daughter cells post-mitotic division is released through budding of ectosomes from flagellar membranes. Instances of such vesicle-like structures pinching off from flagellar membranes in NaCl-induced palmelloids could suggest the presence of VLE (Fig. 3c, d, zoom ins). However, failure in the process of hatching could either be a defence mechanism adopted to protect the *naïve* daughter cells from saline environment or a result of the inactivation of VLE due to high concentrations of NaCl. *C. eugametos* cells in palmelloids undergo division probably at a lower rate as indicated by the multiple cell wall layers around individual cells [49]; while, a similar scenario was reported in *C. applanata* wherein the five-days old palmelloids contained only 8–10 cells [76]. TEM analysis of palmelloids in the current study showed an increment in the number of autophagy vacuoles. Increase in the vacuole volume was reported in *C. applanata* palmelloids induced in response to medium with pH 4.4 [76].

Accumulation of starch and triacylglycerols in *C. reinhardtii* cells under nitrogen depletion stress is a well-established phenomenon [25,77]. Recent studies on algae such as *Dunaliella* [71], *Chlamydomonas moewusii* [2], *C. reinhardtii* [65], *C. mexicana and Scenedesmus obliquus* [63] have shown similar responses when cultured in medium supplemented with NaCl. A comparative study on the effect of calcium, magnesium and NaCl on *Chlorella vulgaris* and *S. obliquus* showed that lipids accumulated maximally in both organisms with NaCl stress [15]. *C. applanata* palmelloids in response to pH 4.4 medium show a decrease in starch volume [76]. Conversely, in comparison to all the earlier reports on palmelloid formation, only the NaCl-inducible palmelloidy showed intracellular accumulation of starch and neutral lipids making it a distinguishing feature. In the current study, a qualitative detection of intracellular starch and neutral lipids aided in understanding the build-up of these reserve carbon sources in the palmelloid cells after 18 h of stress followed by their disappearance due to assimilation during the de-stress phase (Figs. 5a, 6a). After 18 h of stress, the starch as well as the neutral lipid content in the NaCl-stressed cells was found to be ~1.6 fold higher than the untreated cells (Figs. 5b, 6b). These values matched with those reported by Siaut and co-workers [65].

Exopolysaccharide or mucilage secretion is a common phenomenon among various green, red, and blue green algae [8,13,26,35,41,81]. Algal polysaccharides have been studied for their role as potential soil conditioners [5], anti-adhesive agents to treat bacterial infections [16], detoxifiers of heavy metals and radionuclides from contaminated water [7] and antioxidant [4]. Salinity stress-inducible secretion of EPS is well characterized in *Dunaliella salina*; [43] while, it imparts salt tolerance in *Synechocystis* [54]. The current study is the first to report EPS secretion by *C. reinhardtii* cells during salt stress. Staining of palmelloids with ruthenium red showed that the cells were indeed embedded in a self-secreted polymeric matrix (Fig. 7a). Estimation of the EPS concentration in the cell-free medium by Anthrone assay revealed ~5-fold increase with NaCl as compared to untreated cells (Fig. 7b). These values suggest a probable role for NaCl as a modulator in the growth medium for increased EPS production.

4.3. Proteome analysis of the spent medium

The presence of proteins in the cell-free supernatants after stress and de-stress was revealed by one-dimensional PAGE; but, a quantitative insight was obtained by iTRAQ analysis. The most abundant protein after NaCl stress was found to be expansin (Table 1). This protein was first discovered in cucumber hypocotyls catalysing non-enzymatic cell wall extension during acid growth [40]. Consequently, its expression was found to be affected by abiotic stress in many plant systems. In *Zea mays*, a real-time-PCR analysis for β-expansin in 100 mM NaCl-treated leaves and shoots of a salt-resistant hybrid SR03 and a salt-sensitive hybrid, Lector, revealed an up-regulation of these transcripts in the former; while, it was severely impaired in the latter indicating its role in maintenance of growth [14]. Yan and co-workers [80] reported that the expression of an *Arabidopsis* expansin, *AtEXP2*, was essential for seed germination. Further, the *exp2* mutant seeds showed delayed germination in the presence of 100 mM NaCl; while, the *AtEXP2* overexpression line was less sensitive to this stress. *AtEXP2* transcript levels were found to be down-regulated in germinating seeds of the mutant in response to treatment with 100 and 200 mM NaCl signifying that overexpression could bestow salt resistance during seed germination. The first study to investigate the role of an algal homologue of plant expansin was carried out in *Micrasterias denticulata* [74]. *MdEXP2* was found to be localized in cell wall and Golgi-derived vesicles. *MdEXP2-GFP* over-expressing cells showed phenotype indicative of cell wall alterations; thus, exhibiting functional conservancy. The current study is the first to show that NaCl-induced palmelloid formation in *C. reinhardtii* involves cell wall alterations, in particular, loosening with a direct role for expansin in this process. Ferroxidase 1 (FOX1) was another abundant protein after NaCl stress in the current study. This gene is induced by iron deficiency and encodes a ferroxidase involved in a high-affinity iron uptake system [32]. Under hyper-saline conditions, the availability of iron is severely reduced. *D. salina* overcomes this state by over-expressing four major plasma membrane proteins including a multicopper ferroxidase and D-FOX [57]. In the current study a similar mechanism might be used by *C. reinhardtii* cells to surmount iron deficiency during NaCl stress.

Abundance of pherophorins and hydroxyproline-rich glycoprotein post-NaCl stress indicates cell wall alterations in the present study. Another protein with a WSC domain was found to be abundant post stress.

In yeasts, the maintenance of cell wall integrity, under stress, is controlled by a family of five membrane spanning sensors — Wsc1,Wsc2, Wsc3, Mid2 and Mtl1 ([61] and references therein). Deletion mutants for these proteins display varied phenotypes under different stress conditions. A similar role could be played by this *C. reinhardtii* protein with WSC domain in detecting cell wall stress and aiding in resistance to NaCl. A protein with a Kelch motif having a galactose oxidase domain was also found to be highly abundant in NaCl-stressed cell-free supernatants. Proteins with Kelch motifs participate in protein–protein interactions and have diverse locations and functions [1].The enzyme, galactose oxidase catalyses oxidation of D-galactose to its corresponding aldehydes and has been studied as an extracellular or secreted protein [6]. A galactose oxidase mutant, *glxA*$^-$ from *Streptomyces coelicolor* failed to develop aerial hyphae in the presence of 10% sucrose or 250 mM KCl in the growth medium thereby indicating a role of *glxA* in osmotic stress adaptation [37].

The most abundantly up-regulated protein pds was one harbouring a PAN/APPLE like domain. Such proteins are known to mediate protein–protein or protein–carbohydrate interactions [72].Under de-stress, we observe the dissociation of palmelloids to 'free-living' cells, during which the EPSM encasing the cells is also degraded. Hence, a protein with a PAN/APPLE module might be used to facilitate this process. In parallel, two matrix metalloproteinases (MMP13 and MMP3) were found to be up-regulated pds. MMPs are calcium-dependent endopeptidases involved in degradation of extracellular matrix (ECM) [75]. Since degradation of the ECM around the palmelloid cells is essential for their dissociation to a unicellular state, MMPs have been found to be abundant pds. A Fe-assimilating protein 1(FEA1/H43) was found to be significantly abundant pds. This protein has been reported to be the most abundant in the spent medium for high-CO_2 stress acclimatized *C. reinhardtii* cells [3].

4.4. The palmelloid state as a transition to multicellularity

The phylogenetic series of extant Volvocine algae whereby members are ordered by increasing size and cell number from *Chlamydomonas* to *Volvox*, challengingly suggests a simple trajectory for how more complex multicellular forms evolved in this lineage. Although the evolutionary history of morphological and developmental transitions in this lineage is far more complicated, it is clear that the various multicellular forms evolved from an ancestral *Chlamydomonas* cell [10,20,33,52]. Recently, Moulton and Bell [45] studied evolution of multicellularity in *C. reinhardtii* by subjecting it to an artificial selection pressure in the form of centrifugation prior to passage in fresh nutrient medium. Six of the nine *C. reinhardtii* lines showed an increased frequency to exist as a two- or four-celled cluster. Along with these clusters, certain other multicellular forms like flat green aggregates, spherical aggregates and motile aggregates were also obtained in the population; albeit at a very low frequency. Ratcliff and co-workers [60] too induced multicellularity in *C. reinhardtii* cells using settling selection by centrifugation. Clusters formed in this study were different from palmelloids as these contained >100 cells and were not held together by any common parental cell wall. But these clusters secreted an extracellular gelatinous matrix. Also, when transferred to fresh medium, cells in these clusters took ~4 h to activate their flagella and dispersed from the cluster. It was therefore suggested that under centrifugation selection conditions, *C. reinhardtii* exhibits alternating phases in its lifecycle; one being the growth phase wherein the cells form clusters by increasing the cell size; while, the other being the dispersal phase in which the cells reproduce via motile propagules. The simple rule for multicellularity is for single cells to come together, probably as a cluster so as to form a co-operative group. Such a group maintains this co-operation so as to favour division of labour. Above all, factors or conditions that favour co-operation need to be identified [78]. With NaCl as an environmental condition, we believe that the unicellular *C. reinhardtii* vegetative cell tries to divide to form 2^n number of cells; but, the cells are unable to hatch. A failure to hatch is also postulated as the mechanism for the evolution of colonial algae such as *Gonium*, which forms a mat of eight cells, and more complex multicellular genera whose numbers are always powers of two [29]. The palmelloids of *C. reinhardtii* are covered with the extracellular matrix which dissolves only when the stress is relieved. In other words, we conclude that the palmelloid phenotype is a pro-survival strategy adapted by the unicellular green alga, and a stepping stone towards evolving multicellular *Chlamydomonas* ([38]; and the current study).

Supplementary data to this article can be found online at http://dx.doi.org/10.1016/j.algal.2016.03.035.

Acknowledgement

Work in the JSD laboratory and the DKK scholarship was funded by the Department of Atomic Energy, India. JSD and DKK thank Dr. G. K. Rao for guidance in performing the ANOVA test.

References

[1] J. Adams, R. Kelso, L. Cooley, The kelch repeat superfamily of proteins: propellers of cell function, Trends Cell Biol. 10 (2000) 17–24.
[2] S.A. Arisz, T. Munnik, The salt stress-induced LPA response in *Chlamydomonas* is produced via PLA_2 hydrolysis of DGK-generated phosphatidic acid, J. Lipid Res. 52 (2011) 2012–2020.
[3] M. Baba, I. Suzuki, Y. Shiraiwa, Proteomic analysis of high-CO_2-inducible extracellular proteins in the unicellular green alga, *Chlamydomonas reinhardtii*, Plant Cell Physiol. 52 (2011) 1302–1314.
[4] A. Bafana, Characterization and optimization of production of exopolysaccharide from *Chlamydomonas reinhardtii*, Carbohydr. Polym. 95 (2013) 746–752.
[5] W. Barclay, R. Lewin, Microalgal polysaccharide production for the conditioning of agricultural soils, Plant Soil 88 (1985) 159–169.
[6] A. Baron, C. Stevens, C. Wilmot, K. Seneviratnes, V. Blakeley, D. Dooleyf, S. Phillips, P. Knowles, M. McPherson, Structure and mechanism of galactose oxidase.the free radical site*, J. Biol. Chem. 269 (1994) 25095–25105.
[7] J. Bender, P. Phillips, Microbial mats for multiple applications in aquaculture and bioremediation, Bioresour. Technol. 94 (2004) 229–238.
[8] A. Boney, Mucilage: the ubiquitous algal attribute, Br. Phycol. J. 16 (1981) 115–132.
[9] A. Coleman, The Roles of Resting Spores and Akinetes in Chlorophyte Survival, Cambridge University Press, 1983.
[10] A. Coleman, Phylogenetic analysis of "volvocacae" for comparative genetic studies, Proc. Natl. Acad. Sci. 96 (1999) 13892–13897.
[11] J.W. Costerton, K.J. Cheng, G.G. Geesey, T.I. Ladd, J.C. Nickel, M. Dasgupta, T.J. Marrie, Bacterial biofilms in nature and disease, Annu. Rev. Microbiol. 41 (1987) 435–464.
[12] M. Crayton, A comparative cytochemical study of Volvacacean matrix polysaccharides, J. Phycol. 18 (1982) 336–344.
[13] M. El-Sheekh, H. Khairy, R. El-Shenody, Algal production of extra and intra-cellular polysaccharides as an adaptive response to the toxin crude extract of *Microcystis aeruginosa*, Iran. J. Environ. Health Sci. Eng. 9 (2012) 10.
[14] C. Geilfus, C. Neuhaus, K. Mühling, C. Zörb, β-expansins are divergently abundant in maize cultivars that contrast in their degree of salt resistance, Plant Signal. Behav. 6 (2011) 1279–1281.
[15] P.C. Gorain, S.K. Bagchi, N. Mallick, Effects of calcium, magnesium and sodium chloride in enhancing lipid accumulation in two green microalgae, Environ. Technol. 34 (2013) 1887–1894.
[16] M. Guzman-Murillo, F. Ascencio, Anti-adhesive activity of sulphated exopolysaccharides of microalgae on attachment of red sore disease-associated bacteria and *Helicobacter pylori* to tissue culture cells, Lett. Appl. Microbiol. 30 (2000) 473–478.
[17] M. Hanikenne, *Chlamydomonas reinhardtii* as a eukaryotic photosynthetic model for studies of heavy metal homeostasis and tolerance, New Phytol. 159 (2003) 331–340.
[18] E. Harris, The Chlamydomonas Sourcebook. A Comprehensive Guide to Biology and Laboratory Use, Academic Press, San Diego, 1989.
[19] R. Hema, M. Senthil-Kumar, S. Shivakumar, P. Chandrasekhara Reddy, M. Udayakumar, *Chlamydomonas reinhardtii*, a model system for functional validation of abiotic stress responsive genes, Planta 226 (2007) 655–670.
[20] M. Herron, R. Michod, Evolution of Complexity in the Volvocine Algae: Transitions in Individuality Through Darwin's Eye Evolution, Vol. 622008 436–451.
[21] D. Hessen, E. Donk, T. Andersen, Growth responses, P-uptake and loss of flagellae in *Chlamydomonas reinhardtii* exposed to UV-B, J. Plankton Res. 17 (1995) 17–27.
[22] K. Iwasa, S. Murakami, Palmelloid formation of *Chlamydomonas*, Physiol. Plant. 21 (1968) 1224–1233.
[23] K. Iwasa, S. Murakami, Palmelloid formation of *Chlamydomonas* II. Mechanism of palmelloid formation by organic acids, Physiol. Plant. 22 (1969) 43–50.
[24] A. Jamers, W. De Coen, Effect assessment of the herbicide paraquat on a green alga using differential gene expression and biochemical biomarkers, Environ. Toxicol. Chem. 29 (2010) 893–901.
[25] G.O. James, C.H. Hocart, W. Hillier, H. Chen, F. Kordbacheh, G.D. Price, M.A. Djordjevic, Fatty acid profiling of *Chlamydomonas reinhardtii* under nitrogen deprivation, Bioresour. Technol. 102 (2011) 3343–3351.

[26] R. Jones, Extracellular mucilage of the red alga *Porphyridium cruentum*, J. Cell. Comp. Physiol. 60 (1962) 61–64.
[27] A.S. Kaprelyants, J.C. Gottschal, D.B. Kell, Dormancy in non-sporulating bacteria, FEMS Microbiol. Rev. 10 (1993) 271–285.
[28] D. Khona, V. Rao, M. Motiwalla, P. Varma, A. Kashyap, K. Das, S. Shirolikar, L. Borde, J. Dharmadhikari, A. Dharmadhikari, et al., Anomalies in the motion dynamics of long-flagella mutants of *Chlamydomonas reinhardtii*, J. Biol. Phys. 39 (2013) 1–14.
[29] D. Kirk, Volvox, Molecular-Genetic Origins of Multicellularity and Cellular Differentiation, Cambridge University Press, 1998.
[30] U. Klein, Intracellular carbon partitioning in *Chlamydomonas reinhardtii*, Plant Physiol. 85 (1987) 892–897.
[31] Z. Kou, S. Bei, J. Sun, J. Pan, Fluorescent measurement of lipid content in the model organism *Chlamydomonas reinhardtii*, J. Appl. Phycol. 25 (2013) 1633–1641.
[32] S. La Fontaine, J. Quinn, S. Nakamoto, M. Page, V. Go¨hre, J. Moseley, J. Kropat, S. Merchant, Copper-dependent iron assimilation pathway in the model photosynthetic eukaryote *Chlamydomonas reinhardtii*, Eukaryot Cell 1 (2002) 736–757.
[33] A. Larson, M. Kirk, D. Kirk, Molecular phylogeny of the Volvacine Flagellates, Mol. Biol. Evol. 9 (1992) 85–105.
[34] H.K. Ledford, B.L. Chin, K.K. Niyogi, Acclimation to singlet oxygen stress in *Chlamydomonas reinhardtii*, Eukaryot Cell 6 (2007) 919–930.
[35] R. Lewin, Extracellular polysaccharides of green algae, Can. J. Microbiol. 2 (1956) 665–672.
[36] J.W. Lilly, J.E. Maul, D.B. Stern, The *Chlamydomonas reinhardtii* organellar genomes respond transcriptionally and post-transcriptionally to abiotic stimuli, Plant Cell 14 (2002) 2681–2706.
[37] R. Liman, P. Facey, G. Keulen, P. Dyson, R. Sol, A laterally acquired galactose oxidase-like gene is required for aerial development during osmotic stress in *Streptomyces coelicolor*, PLoS One 8 (2013) e54112.
[38] M. Lurling, W. Beekman, Palmelloids formation in *Chlamydomonas reinhardtii*: defence against rotifer predators? Ann. Limnol. Int. J. Limnol. 42 (2006) 65–72.
[39] G. Mastrobuoni, S. Irgang, M. Pietzke, H.E. Assmus, M. Wenzel, W.X. Schulze, S. Kempa, Proteome dynamics and early salt stress response of the photosynthetic organism *Chlamydomonas reinhardtii*, BMC Genomics 13 (2012) 215.
[40] S. McQueen-Mason, D. Durachko, D. Cosgrove, Two endogenous proteins that induce cell wall extension in plants, Plant Cell 4 (1992) 1425–1433.
[41] A. Metaxatos, C. Panagiotopoulos, L. Ignatiades, Monosaccharide and amino acid composition of mucilage material produced from a mixture of four phytoplanktonic taxa, J. Exp. Mar. Biol. Ecol. 294 (2003) 203–217.
[42] D. Miller, I. Mellman, D. Lamport, M. Miller, The chemical composition of the cell wall of *Chlamydomonas gymnogama* and the concept of a plant cell wall protein, J. Cell Biol. 63 (1974) 420–429.
[43] A. Mishra, B. Jha, Isolation and characterization of extracellular polymeric substances from micro-algae *Dunaliella salina* under salt stress, Bioresour. Technol. 100 (2009) 3382–3386.
[44] S. Moharikar, J. D'Souza, A. Kulkarni, B. Rao, Apoptotic-like cell death pathway is induced in unicellular chlorophyte *Chlamydomonas reinhardtii* (chlorophyceae) cells following UV irradiation: detection and functional analyses, J. Phycol. 42 (2006) 423–433.
[45] T. Moulton, G. Bell, Selecting for multicellularity in the unicellular alga *Chlamydomonas reinhardtii*, McGill Sci. Undergr. Res. J. 8 (2013) 30–38.
[46] G.V. Mukamolova, A.S. Kaprelyants, D.B. Kell, M. Young, Adoption of the transiently non-culturable state—a bacterial survival strategy? Adv. Microb. Physiol. 47 (2003) 65–129.
[47] O. Murik, A. Elboher, A. Kaplan, Dehydroascorbate: a possible surveillance molecule of oxidative stress and programmed cell death in the green alga *Chlamydomonas reinhardtii*, New Phytol. 202 (2013) 471–484.
[48] K. Nakamura, M. Sakon, M.K. Hatanaka, Chemical factors affecting palmeloid-forming activity of chloroplatinic acid on *Chlamydomonas eugametos*, Physiol. Plant. 36 (1976) 293–296.
[49] K. Nakamura, D.F. Bray, E.B. Wagenaar, Ultrastructure of *Chlamydomonas eugametos* palmelloids induced by chloroplatinic acid treatment, J. Bacteriol. 121 (1975) 338–343.
[50] S. Nakamura, H. Takino, M. Kojima, Effect of lithium on flagellar length in *Chlamydomonas reinhardtii*, Cell Struct. Funct. 12 (1987) 369–374.
[51] S. Neelam, R. Subramanyam, Alteration of photochemistry and protein degradation of photosystem II from *Chlamydomonas reinhardtii* under high salt grown cells, J. Photochem Photobiol B 124 (2013) 63–70.
[52] H. Nozaki, K. Misawa, T. Kajita, M. Kato, S. Nohara, M. Watanabe, Origin and evolution of the colonial Volvocales (Chlorophyceae) as inferred from multiple, chloroplast gene sequences, Mol. Phylogenet. Evol. 17 (2000) 256–268.
[53] Y. Olsen, G. Knutsen, T. Lien, Characteristics of phosphorus limitation in *Chlamydomonas reinhardtii* (chlorophyceae) and its palmelloids, J. Phycol. 19 (1983) 313–319.
[54] S. Ozturk, B. Aslim, Modification of exopolysaccharide composition and production by three cyanobacterial isolates under salt stress, Environ. Sci. Pollut. Res. Int. 17 (2009) 595–602.
[55] J.D. Parker, L.K. Hilton, D.R. Diener, M.Q. Rasi, M.R. Mahjoub, J.L. Rosenbaum, L.M. Quarmby, Centrioles are freed from cilia by severing prior to mitosis, Cytoskeleton (Hoboken) 67 (2010) 425–430.
[56] J.D. Parker, L.M. Quarmby, *Chlamydomonas fla* mutants reveal a link between deflagellation and intraflagellar transport, BMC Cell Biol. 4 (2003) 11.
[57] Y. Paz, A. Katz, U. Pick, A multicopper ferroxidase involved in iron binding to transferrins in *Dunaliella salina* plasma membranes, J. Biol. Chem. 282 (2007) 8658–8666.
[58] M.M. Perrineau, E. Zelzion, J. Gross, D.C. Price, J. Boyd, D. Bhattacharya, Evolution of salt tolerance in a laboratory reared population of *Chlamydomonas reinhardtii*, Environ. Microbiol. 16 (2014) 1755–1766.
[59] L.M. Quarmby, Y.G. Yueh, J.L. Cheshire, L.R. Keller, W.J. Snell, R.C. Crain, Inositol phospholipid metabolism may trigger flagellar excision in *Chlamydomonas reinhardtii*, J. Cell Biol. 116 (1992) 737–744.
[60] W. Ratcliff, M. Herron, K. Howell, J. Pentz, F. Rosenzweig, M. Travisano, Experimental evolution of an alternating uni- and multicellular life cycle in *Chlamydomonas reinhardtii*, Nat. Commun. 4 (2013).
[61] R. Rodicio, J. Heinisch, Together we are strong — cell wall integrity sensors in yeasts, Yeast 27 (2010) 531–540.
[62] J. Rosenbaum, J. Moulder, D. Ringo, Flagellar elongation and shortening in *Chlamydomonas*. The use of cycloheximide and colchicine to study the synthesis and assembly of flagellar proteins, J. Cell Biol. 41 (1969) 600–619.
[63] S. Salama el, H.C. Kim, R.A. Abou-Shanab, M.K. Ji, Y.K. Oh, S.H. Kim, B.H. Jeon, Biomass, lipid content, and fatty acid composition of freshwater *Chlamydomonas mexicana* and *Scenedesmus obliquus* grown under salt stress, Bioprocess Biosyst. Eng. 36 (2013) 827–833.
[64] N. Shao, C.F. Beck, S.D. Lemaire, A. Krieger-Liszkay, Photosynthetic electron flow affects H_2O_2 signalling by inactivation of catalase in *Chlamydomonas reinhardtii*, Planta 228 (2008) 1055–1066.
[65] M. Siaut, S. Cuine, C. Cagnon, B. Fessler, M. Nguyen, P. Carrier, A. Beyly, F. Beisson, C. Triantaphylides, Y. Li-Beisson, et al., Oil accumulation in the model green alga *Chlamydomonas reinhardtii*: characterization, variability between common laboratory strains and relationship with starch reserves, BMC Biotechnol. 11 (2011) 7.
[66] O.P. Sharma, Textbook of Algae, Tata McGraw-Hill Education, India, 1986.
[67] V. Sirisha, K. Gawade, M. Sinha, J. D'Souza, Programmed cell death is induced by hydrogen peroxide but not by excessive ionic stress of sodium chloride in the unicellular green algae *Chlamydomonas*, Eur. J. Phycol. (2015) (in press).
[68] V. Sirisha, M. Sinha, J. D'Souza, Menadione-induced caspase-dependent programmed cell death in the green chlorophyte *Chlamydomonas reinhardtii*, J. Phycol. 50 (2014) 587–601.
[69] L.H. Stevenson, A case for bacterial dormancy in aquaticsystems, Microb. Ecol. 4 (1978) 127–133.
[70] P. Stragier, R. Losick, Molecular genetics of sporulation in *Bacillus subtilis*, Annu. Rev. Genet. 30 (1996) 297-41.
[71] M. Takagi, Karseno, T. Yoshida, Effect of salt concentration on intracellular accumulation of lipids and triacylglyceride in marine microalgae *Dunaliella* cells, J. Biosci. Bioeng. 101 (2006) 223–226.
[72] H. Tordai, L. Banyai, L. Patthy, The PAN module: the N-terminal domains of plasminogen and hepatocyte growth factor are homologous with the apple domains of the prekallikrein family and with a novel domain found in numerous nematode proteins, FEBS Lett. 461 (1999) 63–67.
[73] L. Valledor, T. Furuhashi, A.M. Hanak, W. Weckwerth, Systemic cold stress adaptation of *Chlamydomonas reinhardtii*, Mol. Cell. Proteomics 12 (2013) 2032–2047.
[74] K. Vannerum, M. Huysman, R. Rycke, M. Vuylsteke, F. Leliaert, J. Pollier, U. Lütz-Meindl, J. Gillard, L. Veylder, A. Goossens, et al., Transcriptional analysis of cell growth and morphogenesis in the unicellular green alga *Micrasterias* (Streptophyta), with emphasis on the role of expansin, BMC Plant Biol. 11 (2011) 1–17.
[75] R. Verma, C. Hansch, Matrix metalloproteinases (MMPs): chemical–biological functions and (Q)SARs, Bioorg. Med. Chem. 15 (2007) 2223–2268.
[76] I. Visviki, D. Santikul, The pH tolerance of *Chlamydomonas applanata* (Volvocales, Chlorophyta), Arch. Environ. Contam. Toxicol. 38 (2000) 147–151.
[77] Z.T. Wang, N. Ullrich, S. Joo, S. Waffenschmidt, U. Goodenough, Algal lipid bodies: stress induction, purification, and biochemical characterization in wild-type and starchless *Chlamydomonas reinhardtii*, Eukaryot Cell 8 (2009) 1856–1868.
[78] S. West, R. Fisher, A. Gardner, E. Kiers, Major evolutionary transitions in individuality, PNAS (2015) 1–8.
[79] C.R. Wood, K. Huang, D.R. Diener, J.L. Rosenbaum, The cilium secretes bioactive ectosomes, Curr. Biol. 23 (2013) 906–911.
[80] A. Yan, M. Wu, L. Yan, R. Hu, I. Ali, Y. Gan, *AtEXP2* is involved in seed germination and abiotic stress response in *Arabidopsis*, PLoS One 9 (2014), e85208.
[81] J.H. Yim, H.K. Lee, Axenic culture of *Gyrodinium impudicum* strain KG03, a marine red-tide microalga that produces exopolysaccharide, J. Microbiol. 42 (2004) 305–314.
[82] C. Yokthongwattana, B. Mahong, S. Roytrakul, N. Phaonaklop, J. Narangajavana, K. Yokthongwattana, Proteomic analysis of salinity-stressed *Chlamydomonas reinhardtii* revealed differential suppression and induction of a large number of important housekeeping proteins, Planta 235 (2012) 649–659.
[83] Z.P. Yordanova, E.J. Woltering, V.M. Kapchina-Toteva, E.T. Iakimova, Mastoparan-induced programmed cell death in the unicellular alga *Chlamydomonas reinhardtii*, Ann. Bot. 111 (2012) 191–205.
[84] Z. Zuo, Y. Zhu, Y. Bai, Y. Wang, Acetic acid-induced programmed cell death and release of volatile organic compounds in *Chlamydomonas reinhardtii*, Plant Physiol. Biochem. 51 (2012) 175–184.